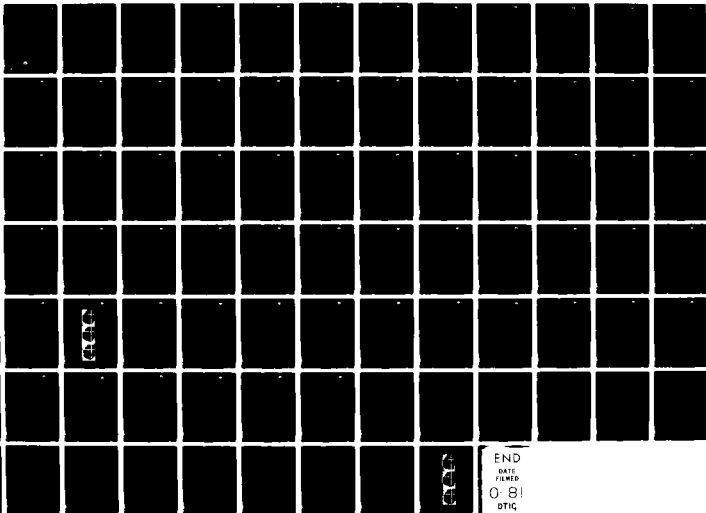


AD-A104 363

ROCKWELL INTERNATIONAL THOUSAND OAKS CA SCIENCE CENTER F/6 7/4
THEORETICAL AND EXPERIMENTAL STUDIES OF THE ELECTRO-OPTIC EFFEC--ETC(U)
AUG 81 M D EWANK, P R NEWMAN N00014-80-C-0498
SC5266.1FR NL

UNCLASSIFIED

1-1
AL
8-04267



END
DATE
FILMED
0-81
DTIC

LEVEL II

12

SC5266.1FR

SC5266.1FR

Copy No. 9

6 THEORETICAL AND EXPERIMENTAL STUDIES OF THE ELECTRO-OPTIC EFFECT: TOWARD A MICROSCOPIC UNDERSTANDING.

FINAL REPORT FOR THE PERIOD June 1980 through May 1981

-31

AD A104363

CONTRACT NO. N00014-80-C-0498

15

Prepared for

Office of Naval Research
Physical Sciences Division
800 North Quincy Street
Arlington, VA 22217

10 M.D. Ewbank
P.R. Newman

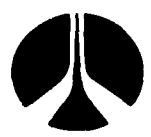
11 AUG 1981

DTIC ELECTRIC
SEP 17 1981
D

12/92

Approved for public release; distribution unlimited

DTIC FILE COPY



Rockwell International
Science Center

81 9 17 089

381 147

UNCLASSIFIED

SECURITY CLASSIFICATION OF THIS PAGE (When Data Entered)

REPORT DOCUMENTATION PAGE		READ INSTRUCTIONS BEFORE COMPLETING FORM
1. REPORT NUMBER	2. GOVT ACCESSION NO.	3. RECIPIENT'S CATALOG NUMBER
	AD-A104363	
4. TITLE (and Subtitle) Theoretical and Experimental Studies of the Electro-Optic Effect: Toward a Microscopic Understanding		5. TYPE OF REPORT & PERIOD COVERED Final Report 06/01/80 through 05/31/81
		6. PERFORMING ORG. REPORT NUMBER SC5266.1FR ✓
7. AUTHOR(s) M.D. Ewbank, P.R. Newman		8. CONTRACT OR GRANT NUMBER(s) N00014-80-C-0498
9. PERFORMING ORGANIZATION NAME AND ADDRESS Rockwell International Science Center 1049 Camino Dos Rios Thousand Oaks, CA 91360		10. PROGRAM ELEMENT, PROJECT, TASK AREA & WORK UNIT NUMBERS NR 372-909 (427)
11. CONTROLLING OFFICE NAME AND ADDRESS Office of Naval Research, Physical Sciences Div. 800 North Quincy Street Arlington, VA 22217		12. REPORT DATE August, 1981
		13. NUMBER OF PAGES 74
14. MONITORING AGENCY NAME & ADDRESS (if different from Controlling Office)		15. SECURITY CLASS. (of this report) Unclassified
		15a. DECLASSIFICATION/DOWNGRADING SCHEDULE
16. DISTRIBUTION STATEMENT (of this Report) Approved for public release: distribution unlimited		
17. DISTRIBUTION STATEMENT (of the abstract entered in Block 20, if different from Report)		
18. SUPPLEMENTARY NOTES		
19. KEY WORDS (Continue on reverse side if necessary and identify by block number) Electro-Optics, optical materials, predictive methodology, bond orbital model, chemical bonds, nonlinear optics, dielectric susceptibilities, bond polarity, electronic and lattice response, ionic displacive, transverse charge, reststrahl vibrations, zincblendes, chalcopyrites, tellurium dioxide, thallium arsenic selenide		
20. ABSTRACT (Continue on reverse side if necessary and identify by block number) The electro-optic effect is investigated both theoretically and experimental- ly. The theoretical approach is based upon W.A. Harrison's "Bond-Orbital Model." The separate electronic and lattice contributions to the second- order, electro-optic susceptibility are examined within the context of this model and formulae which can accommodate any crystal structure are presented. In addition, a method for estimating the lattice response to a low frequency (dc) electric field is outlined. Finally, experimental measurements of the		

DD FORM 1473 1 JAN 73 EDITION OF 1 NOV 65 IS OBSOLETE

UNCLASSIFIED

SECURITY CLASSIFICATION OF THIS PAGE (When Data Entered)

UNCLASSIFIED

SECURITY CLASSIFICATION OF THIS PAGE(When Data Entered)

electro-optic effects in TeO_2 and Tl_3AsAs_3 have been performed and the results of these measurements are presented.

Accession For	
NTIS GRA&I	<input checked="" type="checkbox"/>
DTIC TAB	<input type="checkbox"/>
Unannounced	<input type="checkbox"/>
Justification	
By _____	
Distribution/	
Availability Codes	
Dist	Special
A	

DTIC
SEP 11 1971

UNCLASSIFIED

SECURITY CLASSIFICATION OF THIS PAGE(When Data Entered)



TABLE OF CONTENTS

	Page
1.0 INTRODUCTION.....	1
1.1 Program Objectives.....	1
1.2 Previous Work.....	1
1.3 Accomplishments.....	2
1.4 Technical Issues.....	3
1.5 Report Summary.....	3
2.0 TECHNICAL APPROACH.....	4
2.1 Theoretical.....	4
2.1.1 Electro-optic Coefficients.....	4
2.1.2 Susceptibility.....	6
2.1.3 Units.....	16
2.1.4 Bond Orbital Model.....	20
2.1.4.1 Introduction.....	20
2.1.4.2 Susceptibility.....	20
2.1.4.3 Application to Tetrahedral Compounds.....	28
2.1.4.4 Lattice Dynamics.....	35
2.1.4.5 Symmetry.....	44
2.2 Experimental.....	45
2.2.1 TeO ₂	46
2.2.2 Tl ₃ AsSe ₃	57
3.0 SUMMARY AND RECOMMENDATIONS.....	65
4.0 REFERENCES.....	68



LIST OF ILLUSTRATIONS

<u>Figure</u>	<u>Page</u>
1. Relative motion of Ga cation in a rigid lattice of tetrahedrally coordinated As anions, induced by a field, E_x^{dc}	31
2. Example arrangement of a "free" atom #0 coupled to three "rigid" atoms by springs.....	38
3. TeO_2 electro-optic sample configuration.....	49
4. Laue X-ray photograph of $\langle 100 \rangle$ surface in TeO_2	50
5. Optical set-up for electro-optic measurement in TeO_2	51
6. Interference fringe patterns from electro-optic measurement in TeO_2	52
7. Optical set-up for electro-optic measurement in Tl_3AsSe_3	60
8. Plot of detector intensity vs applied voltage from electro-optic measurement in Tl_3AsSe_3	62

LIST OF TABLES

<u>Table</u>	
1. Numerical Calculations of the Susceptibility Tensors for Various Crystal Symmetries.....	27
2. Evaluation of the Electro-Optic Coefficients, Including the Ionic Displacive Contribution, for some Zinblendes.....	34



FOREWORD

This report to the Office of Naval Research describes both theoretical and experimental efforts carried out under contract N00014-80-C-0498 during the period June 6, 1980 through May 31, 1981. The program was carried out at the Rockwell International Science Center, and was managed by Dr. Paul R. Newman. The principal investigators were Mr. Mark D. Ewbank and Dr. Newman. Prof. Walter A. Harrison of Stanford University was a consultant on the theoretical aspects of the program. Valuable contributions were also made by Dr. Pochi Yeh, Mr. Randolph L. Hall and Dr. M. Khoshnevisan of the Science Center. The contract monitor for the Office of Naval Research was Dr. George Wright.



1.0 INTRODUCTION

1.1 Program Objectives

This program has several long range objectives. The first and perhaps foremost is to achieve a fuller understanding at the microscopic level, of the physics leading to the electro-optic (E-O) effect in solids. A further goal is to generate a completely generalized predictive methodology which takes as its input atomic structure and elemental composition and successfully predicts the electro-optic response for the material.

Additionally, efforts in electro-optic device development programs are currently reaching performance levels limited not by device design, but rather by materials characteristics. It is hoped that some of the future experimental efforts of this program will lead to the successful identification, growth, and characterization of new high performance electro-optic materials, so badly needed by this emerging technology.

1.2 Previous Work

Work that is being carried out under this program has evolved from and is a natural consequence of a Rockwell International IR&D program (Project 864 "Optical Materials") at the Science Center. During FY 1979 and 1980, work was begun in conjunction with Prof. W.A. Harrison of Stanford University, on the application of his "Bond-Orbital Model"¹⁻³ or chemical-bond approach to the prediction of the optical dielectric susceptibility of solids; specifically the indices of refraction of solids. After several initial successes in predicting



SC5266.1FR

the first-order susceptibility, efforts evolved towards second-order "perturbation-response" functions⁴ such as the strain-optic effect and the dc electro-optic (Pockels) effect. That portion of the effort which is specifically oriented toward the electro-optic effect is the basis for this program which was officially funded on June 1, 1980. The remainder of the work on the strain-optic effect, the anomalous dispersion in the birefringence, and other basic optical properties of solids will continue to be carried out at the Science Center under IR&D funding. Clearly, there will be many synergistic advantages both theoretically and experimentally in having such a comprehensive approach to the generic topic of the interaction between light and solids.

1.3 Accomplishments

There have been several significant achievements during the first phase of this project. The theoretical work has progressed to first separating the physical sources of the electro-optic effect into those which result primarily from electronic effects and those associated with lattice dynamics or "ionic-displacive effects." The "Bond-Orbital Model" was then modified so that the electronic contribution to the electro-optic effect could be calculated simply and straightforwardly using "universal atomic" parameters and sums over chemical bonds in the crystallographic unit cell. This theory was tested against TeO_2 and predicted an identically zero electronic contribution to the electro-optic tensor in agreement with Kleinman's⁵ symmetry.

The ionic displacive part was next to be investigated. Here, a further distinction was made between relative motions between ions which do not result in a change in the unit cell dimensions, and those which do. The approach,



SC5266.1FR

although not completely evolved, has been to seek a mechanism for calculating the microscopic atomic "spring constants" and then relating these to some more easily measured bulk properties such as the Reststrahl frequency or bulk elastic constants. It is hoped that this will enable predictions of electro-optic properties to be made with a minimum of experimental materials characterization input.

Finally, the experimental aspect of this program has been quite fruitful. Original characterization measurements of the linear electro-optic effect has been completed in TeO_2 , and begun on another compound: Tl_3AsSe_3 . The studies on this latter compound should be complete by late 1981.

1.4 Technical Issues

The most significant technical issue still to be resolved is the identification of those generalized aspects of atomic configuration and chemical bonds that will allow us to calculate the requisite electronic and lattice responses to external perturbations (electric fields and strains).

1.5 Report Summary

The remainder of this report contains the details of our technical approach and the results for both the theoretical and experimental aspects of this program. Finally, there is a short summary of progress and some of our future efforts. Appendix A is the paper on the experimental efforts on TeO_2 , submitted to the Journal of Applied Physics.



2.0. TECHNICAL APPROACH

2.1 Theoretical

2.1.1 Electro-optic Coefficients

A requirement of any theoretical endeavor is that the theory must include a connection to the experiment. In the case of the electro-optic effect, the measurement gives an electro-optic coefficient, r_{ij} , which is defined by the relation⁶⁻⁸

$$\Delta B_{ij} = \sum_k r_{ijk} E_k \quad (1)$$

or in reduced notation

$$\Delta B_i = \sum_k r_{ik} E_k \quad (2)$$

where ΔB_{ij} is the change in the relative optical dielectric impermeability and E_k is the applied electric field. When the frequency of the perturbing electric field is greater than the piezoelectric response, the crystal is considered to be "clamped" and the measurement gives a constant strain electro-optic coefficient, r_{ijk}^S . Elastic deformation occurs for a low frequency (or dc) perturbing field and this "unclamped" situation leads to a constant stress electro-optic coefficient, r_{ijk}^T . The impermeability is defined by

$$B_{ij} = \frac{\partial E_j}{\partial D_i} = (\epsilon^{-1})_{ij} = \left(\frac{1}{n^2}\right)_{ij} \quad (3)$$



SC5266.1FR

where ϵ_{ij} is a dielectric constant, n refers to a refractive index and ϵ^{-1} is the inverse dielectric tensor.

The change in impermeability with applied field can be easily related to a change in refractive index. Let n_1 be the effective refractive index for a particular set of propagation and polarization directions with no applied electric field. Then let n_2 be the effective index for the same set of propagation and polarization directions but now with the electric field applied. The change in impermeability is

$$\Delta B = \frac{1}{n_2^2} - \frac{1}{n_1^2} = \frac{n_1^2 - n_2^2}{n_1^2 n_2^2} = \frac{(n_1 - n_2)(n_1 + n_2)}{n_1^2 n_2^2} \quad (4)$$

and, in the approximation that $n_1 \approx n_2 \equiv n$ and $n_1 - n_2 \equiv -\Delta n$, it becomes

$$\Delta B = -2\Delta n/n^3 \quad (5)$$

The same result can be achieved from differentiation:

$$\frac{dB}{dn} = \frac{d}{dn} \left(\frac{1}{n^2} \right) = -2n^{-3} \quad (6)$$

The explicit relationships between Δn and ΔB_{ij} have been derived⁸ for optically isotropic, uniaxial and biaxial crystals with the light propagating in an arbitrary direction. For example, in uniaxial crystals, the change in the ordinary refractive index is

$$\Delta n_o = \frac{-n_o^3}{2} \left[\frac{S_2^2 \Delta B_{11} + S_1^2 \Delta B_{22} - 2S_1 S_2 \Delta B_{12}}{S_1^2 + S_2^2} \right] \quad (7)$$



SC5266.1FK

for a propagation direction given by unit vector $\xi = (S_1, S_2, S_3) \neq (0, 0, 1)$. The expression for the change in extraordinary refractive can be written

$$\Delta n_e = \frac{-n_e^3(\text{eff})}{2} \left[\frac{S_1^2 S_2^2 A_{11} + S_2^2 S_3^2 A_{22} + (S_1^2 + S_2^2) A_{33} + 2S_1 S_2 S_3^2 A_{12} - 2S_2 S_3 (S_1 + S_2) A_{23} - 2S_1 S_3 (S_1^2 + S_2^2) A_{13}}{S_1^2 + S_2^2} \right] \quad (8)$$

where $n_e(\text{eff})$ is the effective extraordinary refractive index for the propagation direction $\xi = (S_1, S_2, S_3)$:

$$n_e(\text{eff}) = \frac{n_o n_e}{\sqrt{n_o^2 (S_1^2 + S_2^2) + n_e^2 S_3^2}} \quad (9)$$

Relating the impermeability, and hence the electro-optic coefficient, to a change in refractive index is of fundamental importance because 1) experimentally, one nominally measures this change in the index of refraction as a function of applied electric field and 2) theoretically, one calculates the perturbation of the refractive index due to the applied field.

2.1.2 Susceptibility

Traditionally, the refractive index is related to the microscopic nature of a crystalline solid via the polarizability and susceptibility.⁹ In CGS units

$$n = \sqrt{1 + 4\pi\chi} \quad (10)$$

for isotropic materials in the linear regime. The electro-optic effect can be viewed as one of many nonlinear perturbations to this linear susceptibility; in



SC5266.1FK

particular, it corresponds to a second-order susceptibility. There are many conventions used for representing the nonlinear susceptibility coefficients. One method, which is instructive but not rigorous, is to consider a Taylor's series expansion of the induced polarization, \vec{P} , in terms of the three components of the total electric field, \vec{E}^t ,

$$P_i = \sum_j a_{ij} E_j^t + \frac{1}{2} \sum_{jk} b_{ijk} E_j^t E_k^t + \dots \quad (11)$$

where the expansion has been done about the point $\vec{E}^t = 0$ and it has been assumed that the induced polarization for zero electric field is zero, i.e., $P_i(\vec{E}^t = 0) = 0$. Note that the expansion coefficients are a_{ij} , b_{ijk} , etc. Now let the total electric field be a superposition of two electric fields at frequencies ω_1 and ω_2

$$\vec{E}^t = \vec{E}^{\omega_1} + \vec{E}^{\omega_2} \quad (12)$$

In component form,

$$E_m^t = E_m^{\omega_1} + E_m^{\omega_2} \quad (13)$$

Substituting Eq. (13) into Eq. (11) yields



$$\begin{aligned}
 P_i &= \sum_j a_{ij} (E_j^{\omega_1} + E_j^{\omega_2}) + \frac{1}{2} \sum_{jk} b_{ijk} (E_j^{\omega_1} + E_j^{\omega_2})(E_k^{\omega_1} + E_k^{\omega_2}) + \dots \\
 &= \sum_j a_{ij} E_j^{\omega_1} + \sum_j a_{ij} E_j^{\omega_2} + \sum_{jk} \frac{b_{ijk}}{2} E_j^{\omega_1} E_k^{\omega_1} + \sum_{jk} \frac{b_{ijk}}{2} E_j^{\omega_2} E_k^{\omega_2} \\
 &\quad + \sum_{jk} \frac{b_{ijk}}{2} E_j^{\omega_1} E_k^{\omega_2} + \sum_{jk} \frac{b_{ijk}}{2} E_k^{\omega_1} E_j^{\omega_2} + \dots
 \end{aligned} \tag{14}$$

Since, in the summations over j and k, j and k are only "dummy" indices, it is possible to interchange j and k in the last term and then combine the last two terms by factoring out the electric field

$$\begin{aligned}
 P_i &= \sum_j a_{ij} E_j^{\omega_1} + \sum_j a_{ij} E_j^{\omega_2} + \sum_{jk} \frac{b_{ijk}}{2} E_j^{\omega_1} E_k^{\omega_1} + \sum_{jk} \frac{b_{ijk}}{2} E_j^{\omega_2} E_k^{\omega_2} \\
 &\quad + \sum_{jk} \frac{1}{2} (b_{ijk} + b_{ikj}) E_j^{\omega_1} E_k^{\omega_2} .
 \end{aligned} \tag{15}$$

Now, explicitly include the frequency dependence of the fields:

$$E_m^{\omega_1} = E_m^{(1)} \cos \omega_1 t \tag{16}$$

and

$$E_m^{\omega_2} = E_m^{(2)} \cos \omega_2 t . \tag{17}$$

Substituting Eqs. (16) and (17) into Eq. (15) gives



SC5266.1FR

$$P_i = \sum_j a_{ij} E_j^{(1)} \cos \omega_1 t + \sum_j a_{ij} E_j^{(2)} \cos \omega_2 t + \sum_{jk} \frac{b_{ijk}}{2} E_j^{(1)} E_k^{(1)} \cos^2 \omega_1 t$$

$$+ \sum_{jk} \frac{b_{ijk}}{2} E_j^{(2)} E_k^{(2)} \cos^2 \omega_2 t + \sum_{jk} \frac{1}{2} (b_{ijk} + b_{ikj}) E_j^{(1)} E_k^{(2)} \cos \omega_1 t \cos \omega_2 t$$

Using the trigonometric relations of

$$\cos \alpha \cos \beta = \frac{1}{2} \cos (\alpha + \beta) + \cos (\alpha - \beta) \quad \alpha = \beta \quad \frac{1}{2} \cos (2\alpha) + 1 \quad ,$$

$$P_i = \sum_j a_{ij} E_j^{(1)} \cos \omega_1 t + \sum_j a_{ij} E_j^{(2)} \cos \omega_2 t + \sum_{jk} \frac{b_{ijk}}{4} E_j^{(1)} E_k^{(2)} (\cos 2\omega_1 t + 1)$$

$$+ \sum_{jk} \frac{b_{ijk}}{4} E_j^{(2)} E_k^{(2)} (\cos 2\omega_2 t + 1) + \sum_{jk} \frac{1}{4} (b_{ijk} + b_{ikj}) E_j^{(1)} E_k^{(2)} \cos (\omega_1 + \omega_2) t \quad (18)$$

$$+ \sum_{jk} \frac{1}{4} (b_{ijk} + b_{ikj}) E_j^{(1)} E_k^{(2)} \cos (\omega_1 - \omega_2) t \quad .$$

Expressing P_i as a superposition of its various frequency components, i.e.,

$$P_i = P_i^0 + P_i^{\omega_1} + P_i^{\omega_2} + P_i^{2\omega_1} + P_i^{2\omega_2} + P_i^{\omega_1 - \omega_2} + P_i^{\omega_1 + \omega_2} \quad , \quad (19)$$

these separate components can be written out as

$$P_i^0 = \sum_{jk} \frac{b_{ijk}}{4} (E_j^{(1)} E_k^{(1)} + E_j^{(2)} E_k^{(2)}) \quad ,$$

$$P_i^{\omega_1} = \sum_j a_{ij} E_j^{(1)} \cos \omega_1 t \quad , \quad P_i^{\omega_2} = \sum_j a_{ij} E_j^{(2)} \cos \omega_2 t \quad ,$$

$$P_i^{2\omega_1} = \sum_{jk} \frac{b_{ijk}}{4} E_j^{(1)} E_k^{(1)} \cos 2\omega_1 t \quad , \quad P_i^{2\omega_2} = \sum_{jk} \frac{b_{ijk}}{4} E_j^{(2)} E_k^{(2)} \cos 2\omega_2 t \quad ,$$

$$P_i^{\omega_1 - \omega_2} = \sum_{jk} \frac{1}{4} (b_{ijk} + b_{ikj}) E_j^{(1)} E_k^{(2)} \cos (\omega_1 - \omega_2) t \quad , \quad \text{and}$$

$$P_i^{\omega_1 + \omega_2} = \sum_{jk} \frac{1}{4} (b_{ijk} + b_{ikj}) E_j^{(1)} E_k^{(2)} \cos (\omega_1 + \omega_2) t \quad . \quad (20)$$



SC5266.1FR

By examining the frequency dependences of each of these terms, there is an obvious correspondence to the physical phenomena of optical rectification, second harmonic generation, and sum/difference mixing. In addition, for the special case of $\omega_2 = 0$, the sum and difference mixing terms are equal and correspond to the linear electro-optic (Pockel's) effect, which is an induced polarization at the same frequency as the optical field and is proportional to the dc electric field.

To define the higher order susceptibilities, one can write the induced polarization in terms of increasing powers of electric field:¹⁰

$$P_i = \sum_j \chi_{ij}^{(1)} E_j + \sum_{jk} \chi_{ijk}^{(2)} E_j E_k + \sum_{jkl} \chi_{ijkl}^{(3)} E_j E_k E_l + \dots \quad (21)$$

where $\chi^{(1)}$ is the linear or first-order susceptibility, $\chi^{(2)}$ is the second-order susceptibility, etc. Within this context, the linear Taylor series expansion coefficients are identical to the first-order susceptibility tensor elements. Combinations of the second-order Taylor series expansion coefficients correspond to the second-order susceptibilities. While the above procedure is not completely rigorous, it does provide the appropriate correspondences.

An alternate, but somewhat similar, approach in specifying susceptibilities is to define the i^{th} component of the polarization density vector as the negative of the partial derivative of the total energy density with respect to the i^{th} component of electric field. Then, by expressing the total energy density as a Taylor series expansion in the electric field, the susceptibility coefficients can be related to the derivatives of this total energy density with respect to the various fields. Still another method has been invoked in defin-



SC5266.1FR

ing the second-order susceptibility, which explicitly emphasizes the frequency dependence. A general form of the second-order polarization can be written¹¹

$$P_i(\vec{r}, \omega) = \sum_{jk} \int_{-\infty}^{\infty} \chi_{ijk}^{(2)}(-\omega, \omega', \omega - \omega') E_j(\vec{r}, \omega') E_k(\vec{r}, \omega - \omega') d\omega' \quad (22)$$

where negative frequencies are permitted by assuming $E_j(\vec{r}, \omega) = E_j^*(\vec{r}, -\omega)$.

The specific definitions for three second-order susceptibility are:¹²

$$\text{i) Second Harmonic Generation} \quad P_i^{2\omega} = \sum_{jk} \chi_{ijk}^{2\omega} E_j^{\omega} E_k^{\omega} \quad (23)$$

$$\text{ii) dc Effect (Optical Rectification)} \quad P_i^0 = \sum_{jk} \chi_{ijk}^0 E_j^{\omega} E_k^{\omega} \quad (24)$$

$$\text{iii) Electro-Optic Effect} \quad P_i^{\omega} = \sum_{jk} \chi_{ijk}^{\omega} E_j^0 E_k^{\omega} \quad (25)$$

Note that these second-order susceptibilities are assumed to all be distinct tensor quantities. The symmetry in the subscript indices for the three types of susceptibilities is as follows. Second harmonic generation and optical rectification susceptibilities are symmetric in j and k since interchanging two optical fields of the same frequency is physically insignificant. The electro-optic susceptibility is symmetric in i and k as seen from a quantum mechanical formulation, utilizing the electric dipole approximation, or as seen from a thermodynamics argument. This latter argument can be understood by investigating the following question: "What is the total susceptibility that the optical field 'sees' when the dc field perturbs the first order susceptibility?" The polarization is



$$P_i = \sum_k (x_{ijk}^{(1)} + \sum_j x_{ijk}^{eo} E_j) E_k \quad (26)$$

where $x_{ijk}^{eo} \equiv x_{ijk}^w$ in Eq. (25). For a principal axes coordinate system, $x_{ijk}^{(1)}$ is diagonal. To simplify the total susceptibility, consider the dc field to be along \hat{x} i.e., $E_1^0 = E_x^0$ and $E_2^0 = E_3^0 = 0$. Then

$$\begin{pmatrix} P_1 \\ P_2 \\ P_3 \end{pmatrix} = \begin{pmatrix} [x_{111}^{(1)} + x_{111}^{eo} E_x^0] & x_{112}^{eo} E_x^0 & x_{113}^{eo} E_x^0 \\ x_{211}^{eo} E_x^0 & [x_{222}^{(1)} + x_{212}^{eo} E_x^0] & x_{213}^{eo} E_x^0 \\ x_{311}^{eo} E_x^0 & x_{312}^{eo} E_x^0 & [x_{333}^{(1)} + x_{313}^{eo} E_x^0] \end{pmatrix} \begin{pmatrix} E_1 \\ E_2 \\ E_3 \end{pmatrix} \quad (27)$$

In order that this total susceptibility tensor be symmetric, which is a requirement of thermodynamics, it is necessary that:

$$x_{ijk}^{eo} = x_{kji}^{eo} \quad (28)$$

i.e., the "electro-optic" susceptibility is symmetric in the first and third indices. This implies that the "condensed notation" is obtained by contracting the two indices which do not refer to the dc field. In contrast, for both second harmonic generation and optical rectification, the two indices of the optical fields are "condensed."

Finally, by equating the change in refractive index, due to the electro-optic susceptibility perturbing the linear susceptibility, with the



SC5266.1FR

change in impermeability via the electro-optic coefficient (see Eq. (5)), a direct relation between the second-order, electro-optic susceptibility, χ_{ijk}^{eo} , and the electro-optic coefficient, r_{ijk} , may be obtained. A simple technique for approximating this relation is to write the perturbed refractive index as

$$\begin{aligned} n + \Delta n &= \sqrt{1 + 4\pi\chi^{(1)} + \chi^{eo}E} \\ &= \sqrt{1 + 4\pi\chi^{(1)} \left(1 + \frac{4\pi\chi^{eo}E}{1 + 4\pi\chi^{(1)}}\right)^{1/2}} \\ &= n \left(1 + \frac{4\pi\chi^{eo}E}{n^2}\right)^{1/2} \end{aligned} \quad (29)$$

and then use the binomial expansion on the square root to give

$$n + \Delta n = n \left(1 + \frac{1}{2} \left[\frac{4\pi\chi^{eo}E}{n^2}\right] + \dots\right) \quad (30)$$

Then, by referring to Eq. (5),

$$\Delta n \sim \frac{2\pi\chi^{eo}E}{n} \sim \frac{-n^3\Delta B}{2} \quad (31)$$

which implies that

$$\Delta B \sim \frac{-4\pi\chi^{eo}E}{n^4} \quad (32)$$

and, since $\Delta B \sim rE$ from Eq. (1), one obtains

$$r \sim \frac{-4\pi\chi^{eo}}{n^4} \quad (33)$$

Performing the rigorous matrix inversion required to convert the full susceptibility tensor to the impermeability tensor yields the relation^{7,11,13}



SC5266.1FR

$$r_{ikj} = \frac{-4\pi x_{ijk}^{eo}}{\epsilon_{ii}\epsilon_{kk}} \quad (34)$$

where $\epsilon_{ij} = n_j^2 = 1 + 4\pi x_{ij}^{(1)}$ is the optical dielectric constant. Note that convention implies "condensing" the first and second indices in r_{ikj} while "condensing" the first and third indices in x_{ijk}^{eo} . However, in both cases, the "condensed" indices do not refer to the static electric field. Also, the dielectric constants reflect directions other than that specified by the static field.

Let's verify Eq. (34) for a specific example. Consider symmetry point group 422 with the dc electric field applied in the $\langle 100 \rangle$ direction. Then, from combining Eqs. (2) and (3) and using the electro-optic matrices in Kaminow & Turner,⁷ the perturbed impermeability is

$$B = \begin{pmatrix} 1/n_o^2 \\ 1/n_o^2 \\ 1/n_e^2 \\ 0 \\ 0 \\ 0 \end{pmatrix} + \begin{pmatrix} 0 & 0 & 0 \\ 0 & 0 & 0 \\ 0 & 0 & 0 \\ r_{41} & 0 & 0 \\ 0 & -r_{41} & 0 \\ 0 & 0 & 0 \end{pmatrix} \begin{pmatrix} E_x \\ 0 \\ 0 \end{pmatrix} = \begin{pmatrix} 1/n_o^2 & 0 & 0 \\ 0 & 1/n_o^2 & r_{41}E_x \\ 0 & r_{41}E_x & 1/n_e^2 \end{pmatrix} \quad (35)$$

where n_o is the ordinary index and n_e is the extraordinary index. Referring to Eq. (26), the perturbed susceptibility tensor can be written as

$$\chi = \begin{pmatrix} \chi_o & 0 & 0 \\ 0 & \chi_o & x_{213}^{eo} E_x \\ 0 & x_{312}^{eo} E_x & \chi_e \end{pmatrix} \quad (36)$$



SC5266.1FR

since $\chi_{213}^{e0} = \chi_{312}^{e0} = -\chi_{123}^{e0} = -\chi_{321}^{e0}$ are the only nonzero second-order susceptibilities. Note the χ_0 and χ_e are the linear ordinary and extraordinary susceptibilities, i.e., $n_0^2 = 1 + 4\pi\chi_0$ and $n_e^2 = 1 + 4\pi\chi_e$. From Eqs. (3) and (10),

$$B^{-1} = \begin{pmatrix} 1 & 0 & 0 \\ 0 & 1 & 0 \\ 0 & 0 & 1 \end{pmatrix} + 4\pi \begin{pmatrix} \chi_0 & 0 & 0 \\ 0 & \chi_0 & \Delta\chi \\ 0 & \Delta\chi & \chi_e \end{pmatrix} = \begin{pmatrix} n_0^2 & 0 & 0 \\ 0 & n_0^2 & 4\pi\Delta\chi \\ 0 & 4\pi\Delta\chi & n_e^2 \end{pmatrix} \quad (37)$$

where $\Delta\chi$ has been defined as $\Delta\chi = \chi_{213}^{e0} E_x = \chi_{312}^{e0} E_x$. Using the Gauss-Jordan matrix inversion technique to invert B^{-1} gives

$$B = \begin{pmatrix} \frac{1}{n_0^2} & 0 & 0 \\ 0 & \frac{1}{n_0^2} + \frac{(4\pi\Delta\chi)^2}{n_0^2 n_e^2 - (4\pi n_0 \Delta\chi)^2} & \frac{-4\pi\Delta\chi}{n_0^2 n_e^2 - (4\pi\Delta\chi)^2} \\ 0 & \frac{-4\pi\Delta\chi}{n_0^2 n_e^2 - (4\pi\Delta\chi)^2} & \frac{n_e^2}{n_0^2 n_e^2 - (4\pi\Delta\chi)^2} \end{pmatrix}$$

$$\approx \begin{pmatrix} \frac{1}{n_0^2} & 0 & 0 \\ 0 & \frac{1}{n_0^2} & \frac{-4\pi\Delta\chi}{n_0^2 n_e^2} \\ 0 & \frac{-4\pi\Delta\chi}{n_0^2 n_e^2} & \frac{1}{n_e^2} \end{pmatrix} \quad (33)$$

in the limit that $\Delta\chi$ is small so that terms containing $(\Delta\chi)^n$ where $n > 1$ are taken to be zero. Now, equating the matrix elements in Eqs. (35) and (38) implies that

$$r_{41} E_x = \frac{-4\pi\Delta\chi}{n_0^2 n_e^2}$$



SC5266.1FR

or

$$r_{41} = \frac{-4\pi \chi_{213}}{n_o^2 n_e^2} = \frac{-4\pi \chi_{312}}{n_o^2 n_e^2} \quad (39)$$

which is in exact agreement with Eq. (34).

2.1.3 Units

A recurring problem encountered when dealing with various nonlinear quantities is comparing and converting between MKS and CGS units. It therefore seems appropriate to summarize some of the conventions used in presenting experimental data, along with a few conversion factors.

The experimental electro-optic coefficient, r_{ij} , is generally expressed in the MKS units of (meter/volt), whereas the second harmonic generation coefficient, d_{ij} , has often been given in the "catch-all" units of (esu) and in the MKS units of (meter/volt) or (coulomb/volt²).

The ambiguity of the "esu" can be cleared up by explicitly expressing the esu in CGS units. This ambiguity stems from the multiple definitions for an "esu." That is, 1 esu = 1 statcoulomb for charge, 1 esu = 1 statvolt for potential, 1 esu = 1 statamp for current, etc. For second harmonic generation coefficients (or any other second-order nonlinear coefficient), an "esu" in CGS units is defined as

$$1 \text{ esu} = 1 \frac{\text{statcoulomb}}{\text{statvolt}^2} \quad (40)$$

where 1 statvolt = 2.998×10^2 volts and 1 coulomb = 2.998×10^9 statcoulombs.

Another frequent problem concerning MKS units involves the MKS definition of the permittivity of free space,



SC5266.1FR

$$\epsilon_0 = 8.854 \times 10^{-12} \frac{\text{coulomb}}{\text{newton-meter}^2} \times \left[1 \frac{\text{newton-meter}}{\text{volt}} \right] = 8.854 \times 10^{-12} \frac{\text{coulomb}}{\text{volt-meter}}, \quad (41)$$

for several different reasons. First, it turns out that ϵ_0 is dimensionless and numerically equal to $(4\pi)^{-1}$ when expressed in CGS units:

$$\begin{aligned} \epsilon_0 &= 8.854 \times 10^{-12} \frac{\text{coulomb}}{\text{volt-meter}} \times \left[\frac{2.998 \times 10^9 \text{ statcoulomb}}{\text{coulomb}} \right] \times \left[\frac{2.998 \times 10^2 \text{ volts}}{\text{statvolt}} \right] \\ &\times \left[\frac{1 \text{ meter}}{100 \text{ centimeter}} \right] \times \left[\frac{1 \text{ statvolt-centimeter}}{\text{statcoulomb}} \right] = \frac{1}{4\pi}. \end{aligned} \quad (42)$$

Secondly, there are two conventions for the relation defining the second harmonic generation coefficient. These two relations, referring back to Eq. (23) for comparison, are

$$P_i^{2\omega} = \frac{1}{2} d_{ijk} E_j^\omega E_k^\omega \quad (43)$$

and

$$P_i^{2\omega} = \frac{1}{2} \epsilon_0 d_{ijk} E_j^\omega E_k^\omega \quad (44)$$

where the two indicated second harmonic generation coefficients differ by a factor of ϵ_0 . That is to say,

$$d_{ijk} \left(\frac{\text{coulomb}}{\text{volt}^2} \right) = \epsilon_0 d_{ijk} \left(\frac{\text{meter}}{\text{volt}} \right) \quad (45)$$

Note that other second-order nonlinear coefficients, such as the electro-optic coefficient, which can be expressed in units of (meters/volt), usually do not require this factor of ϵ_0 when converting to other units. (Instead, use the conversion factor $(4\pi\epsilon_0)$ which is dimensionless and equal to unity.)



SC5266.1FR

As a specific numerical example, consider the results of two different second harmonic generation experiments on TeO_2 . The first experiment¹⁴ used Eq. (44) to define d_{14} and reported a value of $|d_{14}| = 0.69 \times 10^{-12}$ m/V. The second experiment¹⁵ used Eq. (43) to define d_{14} and the result was $|d_{14}| = 1.45 \times 10^{-9}$ esu. In order to directly compare these two values, use Eq. (45) on 0.69×10^{-12} m/V value so that the same definitions for the coefficient, d_{14} , is employed and then convert to esu:

$$|d_{14}| = \epsilon_0 (0.69 \times 10^{-12} \text{ m/V}) = 6.1 \times 10^{-24} \frac{\text{coulomb}}{\text{volt}^2} \times \left[\frac{2.998 \times 10^9 \text{ statcoulomb}}{\text{coulomb}} \right] \\ \times \left[\frac{2.998 \times 10^2 \text{ volt}}{\text{statvolt}} \right]^2 \times \left[\frac{1 \text{ esu}}{\text{statcoulomb/statvolt}^2} \right] = 1.6 \times 10^{-9} \text{ esu} \quad (46)$$

which is in reasonable agreement with the other value of 1.45×10^{-9} esu.

The electro-optic coefficient, r_{ij} , the second harmonic generation coefficient, d_{ij} , and the second-order susceptibility, $\chi_{ijk}^{(2)}$, all have the same dimensions, as is evident from Eqs. (25), (34), (43), and (44). Provided that these coefficients are consistently defined, in contrast to the situation in Eqs. (43) - (46), a particular coefficient may be expressed in units of (meter/volt), (coulomb/volt²), (esu), etc. by using the following conversions:

$$\frac{1 \text{ meter}}{\text{volt}} \times \left[4\pi \times 8.854 \times 10^{-12} \frac{\text{coulomb}}{\text{volt-meter}} \right] = 1.113 \times 10^{-10} \frac{\text{coulomb}}{\text{volt}^2} \quad (47)$$

$$\frac{1 \text{ coulomb}}{\text{volt}^2} \times \left[\frac{2.998 \times 10^9 \text{ statcoulomb}}{\text{coulomb}} \right] \times \left[\frac{2.998 \times 10^2 \text{ volt}}{\text{statvolt}} \right] \times \left[\frac{1 \text{ esu}}{\text{statcoulomb/statvolt}^2} \right] \\ = 2.695 \times 10^{+14} \text{ esu} \quad (48)$$



SC5266.1FR

$$\frac{1 \text{ meter}}{\text{volt}} \times \left[\frac{1.113 \times 10^{-10} \text{ coulomb/volt}^2}{\text{meter/volt}} \right] \times \left[\frac{2.645 \times 10^{14} \text{ esu}}{\text{coulomb/volt}^2} \right] = 2.998 \times 10^4 \text{ esu} \quad (49)$$

$$\frac{1 \text{ meter}}{\text{volt}} \times \left[\frac{100 \text{ centimeter}}{\text{meter}} \right] \times \left[\frac{2.998 \times 10^4 \text{ volt}}{\text{statvolt}} \right] = 2.998 \times 10^4 \frac{\text{centimeter}}{\text{statvolt}} \quad (50)$$

where each quantity in the square brackets, [], is dimensionless and has a value of unity. As a numerical example, utilizing these conversion factors, let us determine the electro-optic susceptibility (in esu) for GaAs associated with an experimental electro-optic coefficient of $r_{41} = 1.2 \times 10^{-12} \text{ m/V}$ and a refractive index of $n = 3.60$. Using Eqs. (34) and (49),

$$\chi_{213}^{eo} = -(3.60)^4 (1.2 \times 10^{-12} \text{ m/V}) (2.998 \times 10^4 \frac{\text{esu}}{\text{m/V}}) / 4\pi = -4.8 \times 10^{-7} \text{ esu}. \quad (51)$$

Finally, from a theoretical point of view, the most convenient representation for these dimensions (see BOM section below) is charge³/energy². To be compatible with this form (and, in addition, combining the results from Eqs. (49) and (50)), Eq. (40) can be rewritten as:

$$1 \text{ esu} = \frac{1 \text{ statcoul}}{\text{statvolt}^2} = \frac{1 \text{ centimeter}}{\text{statvolt}} = \frac{1 \text{ statcoulomb}^3}{\text{erg}^2} \quad (52)$$

since 1 statcoulomb = 1 centimeter-statvolt and 1 statvolt = 1 erg/statcoulomb.



2.1.4 Bond Orbital Model

2.1.4.1 Introduction

One form of tight-binding theory, the Bond Orbital Model (BOM), has previously been used to describe numerous electronic and lattice properties of crystalline solids. As originally formulated by Prof. W.A. Harrison of Stanford University, the BOM was applied to tetrahedrally coordinated solids, in particular, to the elemental and zincblende semiconductors.^{1,2} Specifically, this model has been used to calculate the dielectric properties of tetrahedral solids, including the refractive index for the zincblendes¹ and for the chalcopyrites,¹⁶ along with second-order optical susceptibilities for wurtzite and zincblende compounds.¹⁷ Further refinements in the tight-binding parameterization have previously occurred^{18,19} and are still in progress.²⁰ These new sets of parameters do not affect the basic tenets of the BOM formalism itself, but enter only when applying the theory to certain specific cases. The BOM has recently been reviewed in detail and its scope of applicability has been extended to include other crystal symmetries.³

2.1.4.2 Susceptibility

The lowest-order susceptibility can be expressed with the BOM through an expansion of the total energy in the electric field. The second-order susceptibility is then realized by carrying the expansion to one higher order in the electric field. The simplifying concept of the BOM, which permits a "first principles" prediction of the dielectric properties, is the following. By



SC5266.1FR

calculating the change in polarization in each "chemical" bond caused by the optical electrical field, one obtains the total susceptibility by summing up the contributions from each individual bond. When the crystal geometry (i.e., each bond) is perturbed by a dc electric field, the polarization associated with each bond changes. Consequently, the susceptibility is also modified and it is this change in susceptibility with respect to the dc electric field which corresponds to the linear electro-optic (Pockels) effect.

An alternative, but equivalent, procedure is to directly associate the change in polarization per bond due to both the optical and dc electric fields with the second-order susceptibility. In the BOM, the dipole moment, \vec{p} , of each bond is written as

$$\vec{p} = -e\gamma\vec{d}\alpha_p = -e\gamma\vec{d} V_3(V_2^2 + V_3^2)^{-1/2} \quad (53)$$

where e is the electronic charge, γ is the "center-of-gravity" for hybrid orbitals, \vec{d} is the interatomic distance vector between the two bonding atoms, α_p is the "polarity" of the bond, V_2 is the "covalent" bond energy, and V_3 is the "polar" bond energy. With reference to Eq. (22), the first-order susceptibility, $\chi^{(1)}$, is the average change in dipole moment responding to the optical electric field, \vec{E}^{opt} . In addition, the second-order susceptibility, $\chi^{(2)}$, is the average change in dipole moment responding to both \vec{E}^{opt} and the dc electric field, \vec{E}^{dc} . These two susceptibilities can be expressed as derivatives in these electric fields by

$$\chi^{(1)} = \frac{1}{V} \sum_{\text{bonds}} \frac{d\vec{p}}{d\vec{E}^{opt}} \quad (54)$$

and



SC5266.1FR

$$\chi^{(2)} = \frac{1}{v} \sum_{\text{bonds}} \frac{d^2 \vec{p}}{dE_{\text{opt}} dE_{\text{dc}}} \quad (55)$$

where the average has been obtained by systematically summing over each type of bond in the crystal and then dividing by the volume, v , occupied by those bonds.

The derivative of the dipole moment per bond with respect to one or both of the electric fields can be written in terms of partial derivatives of the dipole moment per bond with respect to various BOM parameters or interatomic distance, multiplied by the change in that particular BOM parameter as a function of the appropriate electric field. This is just an application of the chain-rule for partial differentiation.

For example, the derivative in the first-order susceptibility becomes

$$\left(\frac{d\vec{p}}{dE_{\text{opt}}} \right) = \left(\frac{\partial d}{\partial E_{\text{opt}}} \right) \left(\frac{\partial \vec{p}}{\partial d} \right) + \left(\frac{\partial V_2}{\partial E_{\text{opt}}} \right) \left(\frac{\partial \vec{p}}{\partial V_2} \right) + \left(\frac{\partial V_3}{\partial E_{\text{opt}}} \right) \left(\frac{\partial \vec{p}}{\partial V_3} \right) \quad (56)$$

Each partial derivative can be evaluated separately. By making the assumption that the frequency of the optical electric field is high enough so that the lattice cannot respond to it (i.e., greater than the Reststrahl frequency), the interatomic distance can be taken to be independent of the optical electric field. In other words,

$$\left(\frac{\partial d}{\partial E_{\text{opt}}} \right) = 0 \quad (57)$$

Since the covalent energy can be represented as being proportional to the square of the interatomic distance, i.e.,



SC5266.1FR

$$V_2 = \frac{2.16 \hbar^2}{md^2} \quad (58)$$

where \hbar is Planck's constant divided by 2π and m is the electron mass ($\hbar^2/m = 7.62 \text{ eV-Å}^2$), the chain-rule gives

$$\left(\frac{\partial V_2}{\partial E_{\text{opt}}}\right) = \left(\frac{\partial d}{\partial E_{\text{opt}}}\right) \left(\frac{\partial V_2}{\partial d}\right) = \left(\frac{\partial d}{\partial E_{\text{opt}}}\right) \left[\frac{-2V_2}{d}\right] = 0 \quad (59)$$

Therefore, only the "polar" bond energy term in Eq. (56) is nonzero. Evaluating this term yields

$$\left(\frac{\partial \vec{p}}{\partial V_3}\right) = -e\gamma \vec{d} V_2 (V_2^2 + V_3^2)^{-3/2} \quad (60)$$

and

$$\left(\frac{\partial V_3}{\partial E_{\text{opt}}}\right) = -\gamma e \vec{d} \cdot \hat{E}^{\text{opt}}/2 \quad (61)$$

where \hat{E}^{opt} is the unit vector giving the direction of the optical electric field. This last equation results from the change in energy due to the interaction of the dipole with the total electric field. This dipole energy is $-\gamma e \vec{d} \cdot (\hat{E}^{\text{opt}} + \hat{E}^{\text{dc}})/2$. Finally, by substituting Eqs. (57), (59), (60) and (61) into Eq. (56), the first order susceptibility can now be written as

$$\chi_{ij}^{(1)} = \frac{e^2}{2v} \sum_{\text{bonds}} \frac{\gamma^2 V_2^2 d_i (\vec{d} \cdot \hat{E}_j^{\text{opt}})}{(V_2^2 + V_3^2)^{3/2}} \quad (62)$$

where \hat{E}_j^{opt} is a unit vector in the j^{th} direction which represents the optical electric field.



SC5266.1FR

Following a similar procedure for the second-order susceptibility, the derivative of Eq. (56) with respect to the dc electric field becomes

$$\left(\frac{d^2\vec{p}}{dE^{opt}dE^{dc}}\right) = \left(\frac{\partial V_3}{\partial E^{opt}}\right) \left[\left(\frac{\partial \vec{d}}{\partial E^{dc}}\right) \left(\frac{\partial^2 \vec{p}}{\partial V_3 \partial \vec{d}}\right) + \left(\frac{\partial V_2}{\partial E^{dc}}\right) \left(\frac{\partial^2 \vec{p}}{\partial V_3 \partial V_2}\right) + \left(\frac{\partial V_3}{\partial E^{dc}}\right) \left(\frac{\partial^2 \vec{p}}{\partial V_3^2}\right) \right] \quad (63)$$

where any terms involving the variation of interatomic distance with the optical electric field have been dropped. Noting that

$$\left(\frac{\partial V_3}{\partial E^{dc}}\right) = -\gamma e \vec{d} \cdot \hat{E}^{dc} / 2 \quad (64)$$

and

$$\left(\frac{\partial^2 \vec{p}}{\partial V_3^2}\right) = \frac{3e\gamma \vec{d} V_2^2 V_3}{(V_2^2 + V_3^2)^{5/2}} \quad (65)$$

in addition to using Eq. (61), implies that the "electronic" portion of the second-order susceptibility can be written as

$$\chi_{ijk}^{(2)} \text{ (electronic)} = \frac{3e^3}{4V} \sum_{\text{bonds}} \frac{\gamma^3 V_2^2 V_3 d_i (\vec{d} \cdot \hat{E}_j^{dc}) (\vec{d} \cdot \hat{E}_k^{opt})}{(V_2^2 + V_3^2)^{5/2}} \quad (66)$$

This contribution to the second-order susceptibility has been called the "electronic" part since it has been derived from the deformation of the electron distribution in the bond. The deformation of the electron cloud due to both the optical and dc electric fields results in a change in the "polarity" of the bond.

Another contribution to the second-order susceptibility arises from those terms in Eq. (63) which involve the lattice response to the dc field. This "lattice" contribution has been further divided into an "ionic displacive"



SC5266.1FR

part and "piezoelectric/photoelastic" part. The "ionic displacive" component involves only the relative motions of the atoms whereas the "piezoelectric/photoelastic" component allows a piezoelectric strain or bulk lattice distortion. The reason for this last division is to permit compatibility with distinction of a "clamped" or "unclamped" measurement of the electro-optic coefficient. A "clamped" measurement corresponds to a second-order susceptibility which includes only the electronic and the ionic displacive lattice contributions, and not the piezoelectric/photoelastic portion.

The "lattice" contribution to the second-order susceptibility is obtained by combining Eq. (55) with the first two terms of Eq. (63). Evaluating each factor in this latter equation, for which an explicit, simplifying expression can be obtained, implies

$$\left(\frac{\partial^2 \vec{p}}{\partial V_3 \partial d} \right) = - e_Y V_2^2 V_3^2 + V_3^2 \quad (67)$$

$$\left(\frac{\partial^2 \vec{p}}{\partial V_3 \partial V_2} \right) = + e_Y d V_2 V_3^2 - 2 V_3^2 (V_2^2 + V_3^2)^{-5/2} \quad (68)$$

and, just as in Eq. (59),

$$\left(\frac{\partial V_2}{\partial E} \frac{dc}{dc} \right) = \left(\frac{\partial d}{\partial E} \frac{dc}{dc} \right) \left(\frac{\partial V_2}{\partial E} \frac{dc}{dc} \right) = \left(\frac{\partial d}{\partial E} \frac{dc}{dc} \right) \left[\frac{-2V_2}{d} \right] \quad (69)$$

Then, by substituting the above 3 equations along with Eq. (61), the "lattice" contribution to the second-order susceptibility can be written as



$$x_{ijk}^{(2)}(\text{lattice}) = \frac{e^2}{2v} \sum_{\text{bonds}} \frac{\gamma^2 V_2^2}{(V_2^2 + V_3^2)^{5/2}}$$

$$\left[(V_2^2 + V_3^2) \left(\frac{\partial d_i}{\partial E_j^{dc}} \right) + 2(V_2^2 - 2V_3^2) \frac{d_i}{d} \left(\frac{\partial d}{\partial E_j^{dc}} \right) (\vec{d} \cdot \hat{E}_k^{\text{opt}}) \right] \quad (70)$$

where a distinction is made between the magnitude of the interatomic distance vector, d , and the i^{th} component of the interatomic distance vector d_i (i.e., $\vec{d} = \sum_{i=1}^3 d_i \hat{x}_i$). This contribution to the second-order susceptibility is called the "lattice" part since it has been derived from atomic displacements (both relative atomic motions and bulk piezoelectric distortions) due to the dc electric field. In fact, the lattice response to the dc field enters into the formalization as a single factor, $(\partial \vec{d} / \partial E_j^{dc})$, which is the change in the interatomic distance vector with respect to the dc electric field.

In summary, the second-order susceptibility has been described in terms of the Bond Orbital Model. General formulae (Eqs. 62, 66 and 70) have been derived, which permit direct calculation of the first-order susceptibility and the electro-optic, second-order susceptibility for any compound with a known crystal structure. The necessary BOM parameters (V_2 , V_3 and γ) are readily available and the only missing ingredient is the factor that quantifies the lattice response to the dc electric field. Some examples on evaluating this factor are given below. The second-order susceptibility then can be converted to an electro-optic coefficient, r_{ikj} , by using Eq. (34) in conjunction with Eqs. (3), (10), and (62).

A few numerical applications for the first-order susceptibility and the electronic contribution to the second-order susceptibility and electro-optic tensor are illustrated in Table 1. Comparisons with experiment will be



Table 1
Numerical Calculations of The Susceptibility Tensors for Various Crystal Symmetries

Crystal	Pt Grp	$\chi^{(1)}$	n_o, n_e	$\chi^{(2)}$ (electronic) [$\times 10^{-7}$ esu]	r (electronic) [$\times 10^{-12}$ m/V]
GaP (zincblende)	$\bar{4}3m$	$\begin{pmatrix} .648 & 0 & 0 \\ 0 & .648 & 0 \\ 0 & 0 & .648 \end{pmatrix}$	$n_o = n_e = 3.024$	$\begin{pmatrix} 0 & 0 & 0 \\ 0 & 0 & 0 \\ -8.72 & 0 & 0 \end{pmatrix}$	$\begin{pmatrix} 0 & 0 & 0 \\ 0 & 0 & 0 \\ 4.37 & 0 & 0 \end{pmatrix}$
				$\begin{pmatrix} 0 & 0 & 0 \\ 0 & 0 & 0 \\ 0 & -8.72 & 0 \end{pmatrix}$	$\begin{pmatrix} 0 & 0 & 0 \\ 0 & 0 & 0 \\ 0 & 4.37 & 0 \end{pmatrix}$
CdS (wurtzite)	6mm	$\begin{pmatrix} .3736 & 0 & 0 \\ 0 & .3736 & 0 \\ 0 & 0 & .3717 \end{pmatrix}$	$n_o = 2.3866$ $n_e = 2.3867$	$\begin{pmatrix} 0 & 0 & 0 \\ 0 & 0 & 0 \\ 0 & -4.24 & 0 \end{pmatrix}$	$\begin{pmatrix} 0 & 0 & 0 \\ 0 & 0 & 0 \\ 5.47 & 0 & 0 \end{pmatrix}$
				$\begin{pmatrix} 0 & 0 & 0 \\ 0 & 0 & 0 \\ -4.24 & 0 & 0 \end{pmatrix}$	$\begin{pmatrix} 0 & 0 & 0 \\ 0 & 0 & 0 \\ 0 & 5.47 & 0 \end{pmatrix}$
CdGeAs ₂ (chalcopyrite)	$\bar{4}2m$	$\begin{pmatrix} .808 & 0 & 0 \\ 0 & .808 & 0 \\ 0 & 0 & .739 \end{pmatrix}$	$n_o = 3.340$ $n_e = 3.207$	$\begin{pmatrix} 0 & 0 & 0 \\ 0 & 0 & 0 \\ -11.99 & 0 & 0 \end{pmatrix}$	$\begin{pmatrix} 0 & 0 & 0 \\ 0 & 0 & 0 \\ 4.21 & 0 & 0 \end{pmatrix}$
				$\begin{pmatrix} 0 & 0 & 0 \\ 0 & 0 & 0 \\ 0 & -11.99 & 0 \end{pmatrix}$	$\begin{pmatrix} 0 & 0 & 0 \\ 0 & 0 & 0 \\ 0 & 4.21 & 0 \end{pmatrix}$
Tl ₃ AsSe ₃ (sulfosalit)	3m	$\begin{pmatrix} .527 & 0 & 0 \\ 0 & .527 & 0 \\ 0 & 0 & .424 \end{pmatrix}$	$n_o = 2.762$ $n_e = 2.517$	$\begin{pmatrix} -6.03 & 0 & 0 \\ +6.03 & 0 & 0 \\ 0 & -6.70 & 0 \end{pmatrix}$	$\begin{pmatrix} 4.35 & 0 & 5.82 \\ -4.35 & 0 & 5.82 \\ 0 & 0 & 29.29 \end{pmatrix}$
				$\begin{pmatrix} 0 & 0 & 0 \\ -6.70 & 0 & 0 \\ -6.70 & 0 & 0 \end{pmatrix}$	$\begin{pmatrix} 0 & 0 & 0 \\ 5.32 & 0 & 0 \\ 0 & -4.35 & 0 \end{pmatrix}$
TeO ₂	422	$\begin{pmatrix} .276 & 0 & 0 \\ 0 & .276 & 0 \\ 0 & 0 & .206 \end{pmatrix}$	$n_o = 2.114$ $n_e = 1.895$	$\begin{pmatrix} 0 & 0 & 0 \\ 0 & 0 & 0 \\ 0 & 0 & 0 \end{pmatrix}$	$\begin{pmatrix} 0 & 0 & 0 \\ 0 & 0 & 0 \\ 0 & 0 & 0 \end{pmatrix}$



SC5266.1FR

meaningful only when the lattice contribution to the second-order susceptibility is included in the calculation and therefore will be postponed until later.

2.1.4.3 Application to Tetrahedrally Coordinated Compounds

The prescription for calculating susceptibilities, given in the preceding section, has been applied to the binary zincblende compounds. Since all bonds are equivalent, the summations over bonds which appear in Eqs. (62), (66) and (70) can be simplified to give analytic expressions that do not contain any summations. By factoring the BOM parameters out of the summation because they are independent of bond, the summations can be evaluated for the four interatomic distance vectors:

$$\mathbf{d}^{(1)} = (1,1,1) d/\sqrt{3} \quad (71)$$

$$\mathbf{d}^{(2)} = (1,-1,-1) d/\sqrt{3} \quad (72)$$

$$\mathbf{d}^{(3)} = (-1,1,-1) d/\sqrt{3} \quad (73)$$

$$\mathbf{d}^{(4)} = (-1,-1,1) d/\sqrt{3} \quad (74)$$

where $d = \sqrt{3} a/4$ and a is the lattice constant. The summation in Eq. (62) becomes

$$\sum_{4 \text{ bonds}} d_i d_j = \begin{cases} 4d^2/3 & \text{for } i = j \\ 0 & \text{for } i \neq j \end{cases} \quad (75)$$

and the summation in Eq. (66) becomes

$$\sum_{4 \text{ bonds}} d_i d_j d_k = \begin{cases} +4\sqrt{3} d^3/9 & \text{for } i \neq j \neq k \\ 0 & \text{for } i = j \text{ or } i = k \text{ or } j = k \end{cases} \quad (76)$$



SC5266.1FR

However, the choice of signs for the four interatomic distance vectors in Eqs. (71)-(74) was arbitrary. The crystal could have been represented equally well by $\vec{d}^{(1)} = (-1,-1,-1) d/\sqrt{3}$, $\vec{d}^{(2)} = (-1,1,1)d/\sqrt{3}$, $\vec{d}^{(3)} = (1,-1,1)d/\sqrt{3}$ and $\vec{d}^{(4)} = (1,1,-1)d/\sqrt{3}$. Equation (75) is invariant to this sign change but Eq. (76) is not; the right-hand-side of Eq. (76) must be negated. Before dealing with the lattice response necessary to proceed with Eq. (70), the simplified expressions for Eqs. (61) and (66) will now be written as

$$x_{ij}^{(1)} = \begin{cases} \frac{Ne' \gamma^2 V_2^2 d^2}{12(V_2^2 + V_3^2)^{3/2}} & \text{for } i = j \\ 0 & \text{for } i \neq j \end{cases} \quad (77)$$

and

$$x_{ijk}^{(2)} \text{ (electronic)} = \begin{cases} \frac{\sqrt{3} Ne^3 \gamma^3 V_2^2 V_3 d^3}{24 (V_2^2 + V_3^2)^{5/2}} & \text{for } i \neq j \neq k \\ 0 & \text{for } i = j \text{ or } i = k \text{ or } j = k \end{cases} \quad (78)$$

respectively, where $N = 3/v = 4/a^3 = 3\sqrt{3}/16/d^3$ is the electron density (i.e., the number of electrons in four bonds). These two equations agree with Eqs. (4-28) and (5-13) of Reference 3.

In order to simplify Eq. (70), the lattice response in the binary zinc-blendes, induced by a dc electric field, must first be estimated. As the initial step, consider only the ionic displacive portion of the lattice response. Using GaAs as a specific example, the relative motion of a Ga cation, in a dc field, will be determined with respect to a rigid lattice of As anions. This



SC5266.1FR

relative motion is illustrated, in an exaggerated fashion, in Fig. 1 for $\vec{E}^{dc} = E_x^{dc} \hat{x}$. This perturbed interatomic distance vectors can be written as

$$\vec{d}^{(1)} = ([1 - \delta], 1, 1)d/\sqrt{3} \quad (79)$$

$$\vec{d}^{(2)} = ([1 - \delta] -1, -1)d/\sqrt{3} \quad (80)$$

$$\vec{d}^{(3)} = (-[1 + \delta], 1, -1)d/\sqrt{3} \quad (81)$$

$$\vec{d}^{(4)} = (-[1 + \delta], -1, 1)d/\sqrt{3} \quad (82)$$

where $\vec{u} = u\hat{x} = \delta d/\sqrt{3} \hat{x}$ is the relative vector displacement of the Ga cation. By associating two lattice vibrational frequencies with a "classical" spring constant, K ,²¹

$$K = \frac{1}{2} M\omega^2 = \frac{4}{3d^2} (C_0 + 8C_1)$$

where C_0 and C_1 are the "bond-stretching" and "bond-bending" force constants, the displacement can be obtained. The force of the displaced Ga cation is equated with the force exerted by the dc electric field on this cation:

$$\vec{F} = K\vec{u} = ee_T^* \vec{E}^{dc} \quad (83)$$

where \vec{u} is the vector displacement, e is the electronic charge, e_T^* is the dimensionless "transverse" effective charge and \vec{E}^{dc} is the applied dc electric field corrected for the dc surface charges. Solving for the displacement gives

$$\vec{u} = \frac{3ee_T^* E^{dc} d^2}{4(C_0 + 8C_1)} \quad (84)$$

and e_T^* , C_0 and C_1 have been calculated or tabulated in Reference 3.



SC81-14061

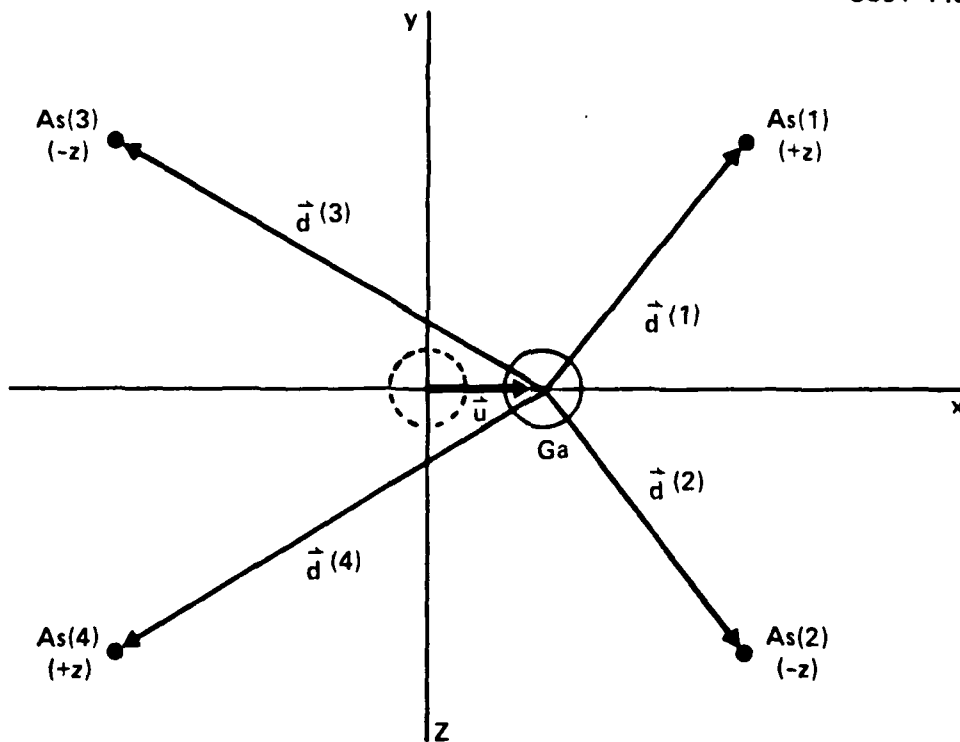


Fig. 1 Relative motion of Ga cation in a rigid lattice of tetrahedrally coordinated As anions, induced by a field, E_x^{dc} .



SC5266.1FR

Now, referring back to Eq. (70) along with Eqs. (79)-(82) and (84), evaluate the lattice response factors $(\partial d_i / \partial E_j^{dc})$ and $(\partial d / \partial E_j^{dc})$ for each of the four bonds. The first factor is

$$\frac{\partial d_i}{\partial E_j^{dc}} = \begin{cases} -\delta d / (\sqrt{3} E_j^{dc}) = -\frac{u_i}{E_j} = \frac{-3ee_1^* d^2}{4(C_0 + 8C_1)} & \text{for } i = j \\ 0 & \text{for } i \neq j \end{cases} \quad (85)$$

which leads to a summation, in the crystal geometry factors in Eq. (70), of

$$\sum_{4 \text{ bonds}} \frac{\partial d_i}{\partial E_j^{dc}} (d \cdot \hat{E}_k^{\text{opt}}) = \begin{cases} \frac{-u_i}{E_j} \sum_{4 \text{ bonds}} d_k & \text{for } i = j \\ 0 & \text{for } i \neq j \end{cases}$$

$$= + 4u_1^2 / E_j^{dc} \quad \text{for } i = j = k \quad (86)$$

$$\approx 0$$

since $\sum_{4 \text{ bonds}} d_k = -4u_j$. This summation is taken to be zero when retaining terms only to first-order in the displacement. To first-order in δ , the second factor becomes

$$\frac{\partial d}{\partial E_j^{dc}} = \frac{d\sqrt{1 \pm 2\delta/3} - d}{E_j^{dc}} \quad (87)$$

where, for example, the - sign is for bonds 1 and 2 while the + sign is for bonds 3 and 4 when $E_j^{dc} = E_x$. By performing a binomial expansion on the squared root,



SC5266.1FR

$$\frac{\partial d}{\partial E_j^{dc}} = (\pm)_j \frac{\delta d}{3E_j^{dc}} = \frac{(\pm)_j |\vec{u}|}{\sqrt{3} E_j^{dc}} = \frac{(\pm)_j \sqrt{3} e e_T^* d^2}{4 (C_0 + 8C_1)} \quad (88)$$

where $|\vec{u}|$ is the magnitude of the displacement. Substituting this into the last term of Eq. (70) gives

$$\sum_{4 \text{ bonds}} \frac{d_i}{d} \frac{\partial d}{\partial E_j^{dc}} (\vec{d} \cdot \hat{E}_k^{opt}) = \frac{\sqrt{3} e e_T^* d}{4 (C_0 + 8C_1)} \sum_{4 \text{ bonds}} (\pm)_j d_i d_k \quad (89)$$

and this last summation reduces to

$$\sum_{4 \text{ bonds}} (\pm)_j d_i d_k = \begin{cases} -4d^2/3 & \text{for } i \neq j \neq k \\ 0 & \text{for } i = j \text{ or } i = k \text{ or } j = k \end{cases} \quad (90)$$

As in Eq. (76), the sign is dependent upon the choice of sign for the four interatomic distance vectors. Finally, by replacing the results of Eqs. (86), (89), and (90) into Eq. (70), the ionic displacive lattice contribution to the second-order susceptibility for zincblendes can be written as

$$\chi_{ijk}^{(2)} (\text{lattice}) = \frac{\sqrt{3} N e^3 e_T^* V_2^2 (V_2^2 - 2V_3^2) d^3}{24 (V_2^2 + V_3^2)^{5/2} (C_0 + 8C_1)} \quad (91)$$

where N is again the electron density. Numerical examples using this last equation along with Eqs. (77) and (78) are presented in Table 2 for the simple tetrahedral solids, which have force constants listed in Table 9-1 and transverse effective charges calculated from Eq. (9-24) of Reference 3.

The BOM susceptibility formulae for the zincblende compounds, i.e., Eqs. (77), (78) and (91), can be readily modified to accommodate the chalcopyrite, abc_2 , crystal structure. In the "quasi-cubic" approximation,¹⁶ the



Table 2
Evaluation of the Electro-Optic Coefficients, Including the
Ionic Displacive Contribution, for Some Zincblends

Zincblende	d [Å]	n	$\chi^{(2)}$ (electronic) [$\times 10^{-7}$ esu]	$\chi^{(2)}$ (ionic displacive) [$\times 10^{-7}$ esu]	r_{41} [$\times 10^{-12}$ m/V]
GaP	2.36	3.024	-8.72	+0.38	+4.19
GaAs	2.45	3.326	-12.50	+0.68	+4.05
InSb	2.81	3.882	-31.90	+0.72	+5.75
ZnS	2.34	2.130	-4.23	-0.82	+10.28
CuCl	2.34	1.59	-1.59	-0.79	+15.57
CuBr	2.49	1.68	-2.42	-1.22	+19.22
CuI	2.62	1.84	-4.07	-1.12	+18.79



SC5266.1FK

chalcopyrite is regarded as being a zincblende with two different types of bonds. Then, the summations over bonds in Eqs. (62), (66), and (70) reduce to two terms instead of a single term; one for a-c bonds and another for the b-c bonds. Each of these two terms is evaluated separately using the appropriate set of BOM parameters and interatomic distance which characterize the corresponding bond. For example, the first-order susceptibility of Eq. (77) becomes

$$x_{ij}^{(1)} = \begin{cases} \frac{Ne^2}{24} \left[\frac{\gamma^2 V_2^2 d^2}{(V_2^2 + V_3^2)^{3/2}} \Big|_{a-c} + \frac{\gamma^2 V_2^2 d^2}{(V_2^2 + V_3^2)^{3/2}} \Big|_{b-c} \right] & \text{for } i = j \\ 0 & \text{for } i \neq j \end{cases} \quad (92)$$

The second-order susceptibilities can similarly be written as two terms with the leading numeric factor being halved to compensate for the separation of the contributions from the two types of bonds. The "quasi-cubic" approximation leads an isotropic first-order susceptibility, i.e. $x_{11}^{(1)} = x_{22}^{(1)} = x_{33}^{(1)}$. Likewise, the second-order susceptibility has $(x_{123}^{(2)} = x_{321}^{(2)}) = (x_{213}^{(2)} = x_{312}^{(2)}) = x_{132}^{(2)} = x_{231}^{(2)}$. If the actual symmetry of the chalcopyrite structure ($\bar{4}2m$) is employed in Eqs. (62), (66), and (70), then the degeneracies in the susceptibilities are broken: $x_{11}^{(1)} = x_{22}^{(1)} \neq x_{33}^{(1)}$ and $(x_{123}^{(2)} = x_{321}^{(2)}) = (x_{213}^{(2)} = x_{312}^{(2)}) \neq x_{132}^{(2)} = x_{231}^{(2)}$.

2.1.4.4 Lattice Dynamics

General formulae, which can be used to determine the first- and second-order susceptibility tensors, have been given in Eqs. (62), (66), and (70). All three of these formulae require a knowledge of i) the crystal geometry which



SC5266.1FR

specifies the interatomic distance vectors and ii) the BOM parameters that characterize each type of bond. In addition, the last formulae (Eq. 70) requires a knowledge of iii) the lattice response to a dc electric field. The purpose of this section is to provide one detailed procedure for evaluating this latter lattice response factor, $(\partial d / \partial E_j^{dc})$.

The approach taken here is intended to give only the ionic displacive contribution to the lattice response. Hence, the calculated electro-optic coefficients should be compared with "clamped" electro-optic measurement.

Briefly, the method may be outlined as follows. Consider an isolated atom (#0), which is free to move in response to a "dc" electric field, surrounded by a rigid lattice of N neighboring atoms (#1, 2, ... N). Let atom #0 be coupled to each of these fixed neighboring atoms by a classical spring, which is characterized by the spring constant, K_i , where $i = 1, 2, \dots N$. For small displacements, the relative motion of atom #0 with respect to the rigid lattice can be determined by equating the force, which the electric field exerts on the effective charge of atom #0, with the force that the N springs exert on atom #0 when it is displaced from equilibrium. The spring constants are quantified by treating atom #0 as a simple harmonic oscillator and solving the equation of motion for frequencies and normal modes of vibration. By associating the frequencies of vibration with the IR absorption (Reststrahl) frequencies, the spring constants are determined.

In order to specify the problem in more detail, let \vec{r}_0 be the vector to the equilibrium position of atom #0, let \vec{r} be the vector to the displaced position of atom #0, let \vec{u} be the vector displacement, and let \vec{r}_i be the vector



SC5266.1FR

to the fixed position of atom #i ($i = 1, 2, \dots N$), as illustrated in Fig. 2 for $N = 3$. Assuming that all springs are unstretched when atom #0 is at its equilibrium position, the force, \vec{F}_i , on atom #0 due to the i^{th} spring is

$$\vec{F}_i = -K_i (|\vec{r}_i - \vec{r}| - |\vec{r}_i - \vec{r}_0|) \left[\frac{\vec{r}_i - \vec{r}}{|\vec{r}_i - \vec{r}|} \right] \quad (93)$$

where $|\vec{r}_i - \vec{r}_0|$ is the unstretched length of the i^{th} spring, $|\vec{r}_i - \vec{r}|$ is the stretched length, $(|\vec{r}_i - \vec{r}| - |\vec{r}_i - \vec{r}_0|)$ is the amount of stretch in the i^{th} spring, and $(\vec{r}_i - \vec{r})/|\vec{r}_i - \vec{r}|$ is the direction of the restoring force for the i^{th} spring. Note: defining the restoring force as being directed from the displaced position of atom #0 to the fixed position of atom #i assumes that the spring "connections" to the atoms are free to pivot.

When the dc electric field is zero, the equation of motion for atom #0 is

$$m_0 \frac{d^2 \vec{r}}{dt^2} + \sum_{i=1}^N K_i (|\vec{r}_i - \vec{r}| - |\vec{r}_i - \vec{r}_0|) \frac{\vec{r}_i - \vec{r}}{|\vec{r}_i - \vec{r}|} = 0 \quad (94)$$

where m_0 is the mass of atom #0. The simple form of this differential equation results from the assumption of an isolated atom coupled to a rigid lattice. If a spring which connects two atoms, both "free" to respond to external influences, is included, then a more complicated set of coupled differential equations must be solved. The displaced position of atom #0 is related to the equilibrium position by

$$\vec{r} = \vec{r}_0 + \vec{u} \quad (95)$$

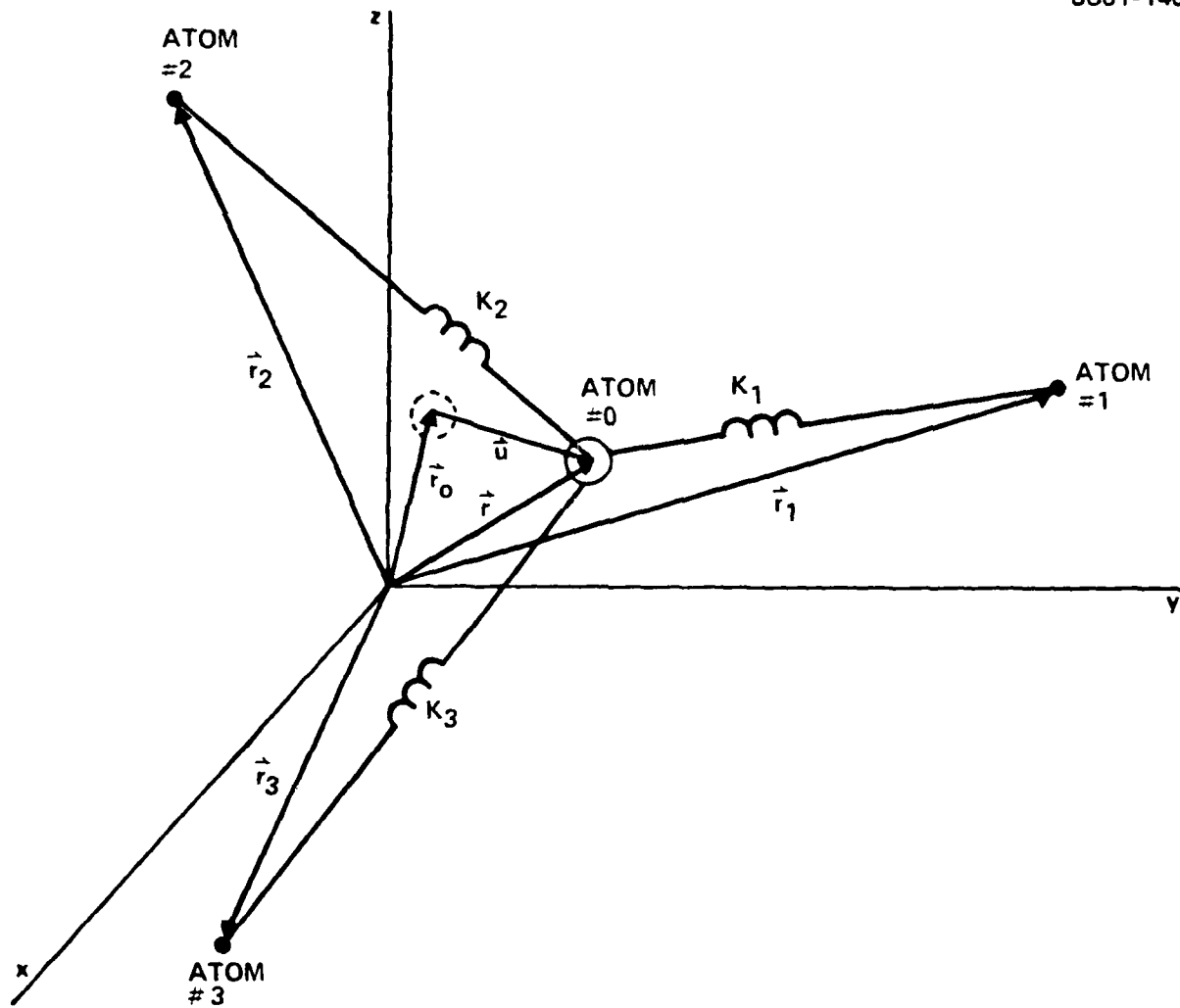


Fig. 2 Example arrangement of "free" atom #0 coupled to three "rigid" atoms by springs.



SC5266.1FR

and it is the vector displacement \vec{u} which undergoes simple harmonic motion.

That is,

$$\vec{u}(t) = \vec{u}_0 \cos(\omega t + \phi) \quad (96)$$

and therefore

$$\frac{d^2 \vec{r}}{dt^2} = \frac{d^2 \vec{r}_0}{dt^2} + \frac{d^2 \vec{u}}{dt^2} = 0 - \omega^2 \vec{u} \quad (97)$$

where $\vec{u} = \Delta x \hat{x} + \Delta y \hat{y} + \Delta z \hat{z}$ is a small quantity. Then, the equation of motion becomes

$$-m_0 \omega^2 (\vec{r} - \vec{r}_0) + \sum_{i=1}^3 K_i \left[1 - \frac{|\vec{r}_i - \vec{r}_0|}{|\vec{r}_i - \vec{r}|} \right] (\vec{r}_i - \vec{r}) = 0 \quad (98)$$

This equation represents a set of nonlinear differential equations which are coupled in the three unknowns, Δx , Δy , and Δz .

The nonlinear factor in Eq. (98) can be linearized in the following way.

Let $d_{i0} = |\vec{r}_i - \vec{r}_0|$ which implies that $d_{i0} = \sqrt{(x_i - x_0)^2 + (y_i - y_0)^2 + (z_i - z_0)^2}$. Then, the \hat{x} -component of the nonlinear factor in Eq. (98) can be written as

$$\begin{aligned} \frac{|\vec{r}_i - \vec{r}_0|}{|\vec{r}_i - \vec{r}|} (x_i - x) &= \frac{d_{i0} (x_i - x_0 - \Delta x)}{\sqrt{(x_i - x_0 - \Delta x)^2 + (y_i - y_0 - \Delta y)^2 + (z_i - z_0 - \Delta z)^2}} \\ &= \frac{(x_i - x_0 - \Delta x)}{\sqrt{1 - \left(\frac{\Delta z}{d_{i0}}\right)^2 [(x_i - x_0)\Delta x + (y_i - y_0)\Delta y + (z_i - z_0)\Delta z]}} \end{aligned}$$

where only term in first order in Δx , Δy and Δz have been retained. By using the binomial expansion on the denominator, this nonlinear factor becomes



SC5266.1FR

$$\frac{|\vec{r}_i - \vec{r}_0|}{|\vec{r}_i - \vec{r}|} (x_i - x) = (x_i - x_0 - \Delta x) + \frac{1}{d_{i0}^2} \left[(x_i - x_0)^2 \Delta x + (x_i - x_0)(y_i - y_0) \Delta y + (x_i - x_0)(z_i - z_0) \Delta z \right] \quad (99)$$

Finally, the linearized equation of motion can be written as

$$+ m_0 \omega^2 \vec{u} + \sum_{i=1}^N \frac{K_i}{|\vec{r}_i - \vec{r}_0|^2} \left[(\vec{r}_i - \vec{r}_0) \{ (\vec{r}_i - \vec{r}_0) \cdot \vec{u} \} \right] = 0 \quad (100)$$

which is an eigenvalue equation in the displacement variable, \vec{u} .

By diagonalizing the matrix, A, whose elements are given by

$$A_{mn} = \sum_{i=1}^N \frac{-K_i}{|\vec{r}_i - \vec{r}_0|^2} (\vec{r}_i - \vec{r}_0)_m (\vec{r}_i - \vec{r}_0)_n \quad (101)$$

the eigenvalues, $m_0 \omega^2$, are determined and, hence, the three frequencies are associated with the three normal modes of vibration for a given set of spring constants, K_i ($i = 1, 2, \dots, N$). An appropriate set of spring constants can be found numerically by using iteration techniques, in which the K_i 's are varied the eigenfrequencies obtained match the experimentally observed lattice optical phonon frequencies.

Once the spring constants are known, the "dc" electric field can be applied and the force exerted by this electric field will exactly balance the forces of the springs on atom #0. Specifically, again linearizing the forces of the springs (see Eq. (99)), we obtain

$$e e_1^* \vec{E}^{dc} = + \sum_{i=1}^N \frac{K_i}{|\vec{r}_i - \vec{r}_0|^2} (\vec{r}_i - \vec{r}_0) \{ (\vec{r}_i - \vec{r}_0) \cdot \vec{u} \} \quad (102)$$



SC5266.1FR

where e_j^* is the effective transverse charge. Solving this equation for the displacement vector, \vec{u} , will result in the determination of the ionic displacive lattice response factor, $(\partial \vec{d} / \partial E_j^{dc})$.

Initial steps have been taken in applying the above procedure to TeO_2 . Since the tellurium atoms are much heavier than the oxygen atoms, assuming that the tellurium atoms form a "rigid" lattice is probably a reasonable approximation. Using the details from the crystal structural determination,²² consider an oxygen with an equilibrium vector position (in coordinate units of Å) of $\vec{r}_0 = (0.63, 1.29, 1.39)$. Its "first" nearest neighbor tellurium atoms are located at $\vec{r}_1 = (0.10, 0.10, 0.00)$ and $\vec{r}_2 = (2.30, 2.49, 1.91)$, which correspond to $d_{10} = 1.92$ Å and $d_{20} = 2.09$ Å, respectively. The bond angle between the oxygen and these two tellurium atoms is 140.8° , which differs considerably with the 169° suggested in Reference 22.

Coupling the oxygen atom to only these two tellurium atoms is not sufficient to constrain the oxygen to the specified equilibrium position. At least one additional coupling must be included for the equilibrium position to be uniquely determined. The next nearest neighbors to oxygen atom #0 are two pairs of oxygen atoms. One pair has an interatomic distance of 2.65 Å and the other pair is 2.75 Å away. However, utilizing any of these four oxygen-oxygen couplings would complicate Eq. (94); that is Eq. (94) would become a coupled differential equation since the motion of one oxygen atom would now depend on the variable positions of other oxygen atoms.

In order to maintain the uncoupled form of Eq. (94), oxygen atom #0 must be viewed as interacting only with tellurium atoms. Therefore, the third



SC5266.1FR

coupling is made to the next nearest tellurium atom, located at $\vec{r}_3 = (-0.10, -0.10, 3.81)$ with $d_{30} = 2.90$ Å. The spring between this tellurium atom and oxygen atom #0 might be considered as a "collective" spring, representing the coupling between oxygen atom #0 and all other neighbors except tellurium atoms #1 and #2.

The infrared frequencies of vibration in TeO_2 have been determined from reflectivity and Raman spectra.²³ The two highest energy modes should correspond to the longitudinal and transverse motions of oxygen #0 with respect to telluriums #1 and #2. The experiment²³ has a pair of high energy modes for both the longitudinal and transverse cases. The longitudinal frequencies are 812 and 720 cm^{-1} whereas the transverse frequencies are 769 and 643 cm^{-1} . The simplified model assumed above would have these pairs of frequencies appear degenerate. Therefore, for the purpose of determining the spring constants in TeO_2 , the geometric mean of these pairs of frequencies is used, giving longitudinal and transverse modes which correspond to $764.6 \text{ cm}^{-1} = 13.1\mu$ and $703.2 \text{ cm}^{-1} = 14.2\mu$, respectively. Note that the geometric mean is employed instead of the arithmetic average since the former can be done in frequency or wavelength and give consistent results, whereas the latter can not.

In order to simplify the fitting procedure of the spring constants, the two springs between oxygen atom #0 and tellurium atoms #1 and #2 are assumed to be characterized by the same spring constant, even though the interatomic distances are slightly different. Then, by obtaining the eigenvalues corresponding to the matrix specified by Eq. (101) for any given set of spring constants, a reasonable fit to the experimental absorption frequencies was accomplished. The set of spring constants, $K_1 = K_2 = 197 \text{ g/sec}^2$ and $K_3 = 270 \text{ g/sec}^2$, yield



SC5266.1FR

absorptions at $761.6 \text{ cm}^{-1} = 13.13\mu$, $699.3 \text{ cm}^{-1} = 14.30\mu$ and $169.9 \text{ cm}^{-1} = 58.86\mu$. The highest energy vibration (13.13μ) is identified as a longitudinal mode since the corresponding eigenvector is only 6.6° away from being parallel to the interatomic distance vector between tellurium atoms #1 and #2. The other two modes (14.30μ and 58.86μ) are transverse because their corresponding eigenvectors are nearly perpendicular to this tellurium interatomic distance vector, deviating by 6.6° and 0.6° respectively. The lowest energy absorption (58.86μ) can also be compared with the experiment.²³ There does exist a transverse mode at $174 \text{ cm}^{-1} = 57.5\mu$ which agrees rather well with the calculated value.

The final step of determining the displacement of oxygen atom #0 in response to a "dc" electric field is complicated by the fact that the transverse effective charge in Eq. (102) is dependent upon the direction of displacement in addition to the crystal structure. This dependence has been evaluated for a few specific crystal structures,³ and a general solution will be obtained in the follow-on to this contract. Until the transverse effective charge is determined, the ionic displacive contribution to the second-order susceptibility cannot be calculated in TeO_2 . Furthermore, the sensitivity of the displacement vector with respect to the "collective" spring constant needs investigation. But this too requires an evaluation of the transverse effective charge and, hence, will be postponed to a later date.

One last comment can be made regarding the applicability of this lattice dynamics model. The relative motion in zincblende compounds suggested by Fig. 1 should be adequately described by Eqs. (93) - (102). Consequently, an alternate expression to Eq. (91) may be obtained which depends directly on the



SC5266.1FR

infrared absorption frequencies rather than the force constants, C_0 and C_1 . Presumably, these experimental absorption frequencies are more readily available than the latter force constants for the zincblende compounds. Additionally, the similar ionic displacive motion that occurs in the chalcopyrites should also be accommodated by Eqs. (93) - (102) by permitting distinct springs between a-c and b-c atom pairs.

2.1.4.5 Symmetry

The symmetries of the calculated first- and second-order susceptibility tensors, determined by the summations over bonds in Eqs. (62), (66) and (70) of various combinations of interatomic distance vectors, must reflect the symmetry of the lattice. This point was illustrated for the zincblende structure in Eqs. (75), (76), (86), (89) and (90). The symmetry requirements on the second-order susceptibility are specified by the point group symmetry.⁷ And as mentioned previously, thermodynamics requires the first-order susceptibility to be symmetric. The formulae associated with the BOM must fulfill these symmetry requirements.

Examining the first-order susceptibility expression, Eq. (62), it is obvious that the crystal geometric factor for each bond, $d_i d_j$, is symmetric in i and j . Therefore, the summation over bonds is also symmetric in i and j . The electronic contribution to the second-order susceptibility, Eq. (66), is almost as simple. The crystal geometric factor for each bond can be written as $d_i d_j d_k$, which is symmetric in i , j and k , as is the summation over bonds. However, Kleinman's symmetry⁵ implies that the second-order susceptibility coefficients, arising from electronic processes where there is no absorption or dispersion,



SC5266.1FR

are symmetric in all three indices. Consequently, the BOM electronic contribution to the second-order susceptibility is seen to be consistent with Kleinman's symmetry condition. Finally, no general statement can be made, at this time, concerning the symmetry of the crystal geometric factors in Eq. (70), which describe the lattice contribution to the second-order susceptibility. Presumably, as indicated in Eq. (28), these factors will turn out to be symmetric in i and k only.

2.2 Experimental

The experimental efforts in this program have focussed on two materials: TeO_2 (tellurium dioxide or paratellurite) and Tl_3AsSe_3 (thallium arsenic selenide or TAS). In much the same manner as was shown in the theory, we have chosen materials in which we hope to be able to experimentally separate the electronic and ionic contributions to the E-0 effect. TAS is a ternary chalcogenide semiconductor with a moderate bandgap of $\sim 1\text{eV}$. Although there is some evidence of soft mode behavior²⁴ in this system, it is thought that the dominant mechanism in TAS is the electronic response. TeO_2 possesses characteristics that suggest comparable contributions from both effects to the E-0 response. Being a well known acousto-optic material,²⁵ TeO_2 exhibits a soft mode phase transition²⁶ under moderate pressure ($\sim 9\text{ K bars}$). Additionally TeO_2 has a reasonably high $c(\infty)$ of approximately 4 and an $\epsilon(0)$ of about 25. Our experimental efforts in Tl_3AsSe_3 to date have been of a rather preliminary nature and will be completed during the next few months. The TeO_2 work has progressed much more quickly and is essentially complete (see Appendix A) at present.



SC5266.1FR

2.2.1 TeO₂

The point group symmetry²² of TeO₂ is tetragonal: 422. This implies that the material is optically uniaxial and has only two non-zero electro-optic coefficients ($r_{41} = -r_{52}$).⁷ TeO₂ is also weakly piezoelectric having one non-zero piezoelectric coefficient²⁷ $d_{11} = 8.13 \times 10^{-12}$ C/N, indicating there is considerable response of the lattice to the presence of a dc electric field. Although Kleinman's symmetry⁵ suggest that materials having the symmetry of 422 should have no non-zero second-order susceptibility coefficients, the underlying assumption of Kleinman's formalism make it inappropriate when one of the electric fields is dc ($\omega = 0$), as is pointed out above (see Theory). In any case, experiments^{14,15,28,29} have shown that there is an apparent "violation" of Kleinman's symmetry in TeO₂ even at optical frequencies (both electric fields have $\omega \neq 0$). We shall, therefore, examine the details of the dc E-0 effect in this material.

If light is propagated along the $\langle 011 \rangle$ direction, the two normal modes occur with the polarization along $\langle 100 \rangle$ (ordinary) and along $\langle 0\bar{1}1 \rangle$ (extraordinary). The impermeability tensor becomes:

$$B = \begin{pmatrix} \frac{1}{n_o^2} & 0 & -r_{41}E_y \\ 0 & \frac{1}{n_o^2} & +r_{41}E_x \\ -r_{41}E_y & +r_{41}E_x & \frac{1}{n_e^2} \end{pmatrix} \quad (103)$$

If we write the polarization vector:

$$P = (l_x \ l_y \ l_z) \quad (104)$$



where ϵ_j = the polarization direction cosines, we can calculate the dielectric response by:

$$\frac{1}{n^2} = R = P(B)P =$$

$$(\epsilon_x \ \epsilon_y \ \epsilon_z) \begin{pmatrix} \frac{1}{n_o^2} & 0 & -r_{41}E_y \\ 0 & \frac{1}{n_o^2} & r_{41}E_x \\ -r_{41}E_y & r_{41}E_x & \frac{1}{n_e^2} \end{pmatrix} \begin{pmatrix} \epsilon_x \\ \epsilon_y \\ \epsilon_z \end{pmatrix} \quad (105)$$

Now in particular for $E = E_x$, and $P = (100)$, which is the ordinary polarization:

$$R = (1 \ 0 \ 0) \begin{pmatrix} \frac{1}{n_o^2} & 0 & 0 \\ 0 & \frac{1}{n_o^2} & r_{41}E_x \\ 0 & r_{41}E_x & \frac{1}{n_e^2} \end{pmatrix} \begin{pmatrix} 1 \\ 0 \\ 0 \end{pmatrix} = \frac{1}{n_o^2} \quad (106)$$

Therefore, $n = n_o$ and the ordinary index is unaffected by the electric field.

If we now let $P = 1/\sqrt{2}(0 \ -1 \ 1)$, which is the extraordinary polarization:

$$\frac{1}{n_e^2(\text{eff})} = R = \frac{1}{\sqrt{2}} (0 \ -1 \ 1) \begin{pmatrix} \frac{1}{n_o^2} & 0 & 0 \\ 0 & \frac{1}{n_o^2} & r_{41}E_x \\ 0 & r_{41}E_x & \frac{1}{n_e^2} \end{pmatrix} \frac{1}{\sqrt{2}} \begin{pmatrix} 0 \\ -1 \\ 1 \end{pmatrix}$$

$$= \frac{1}{2} \left[\frac{1}{n_o^2} - 2r_{41}E_x + \frac{1}{n_e^2} \right] \quad (107)$$



SC5266.1FR

where $n_e(\text{eff})$ is the effective extraordinary index for a propagation direction of $\langle 011 \rangle$. Thus it is only the extraordinary index (or mode) that is affected for our particular choice of the crystal cut which is shown in Fig. 3.

An experimental sample which utilized the interaction geometry shown in Fig. 3 was constructed from TeO_2 single crystal material that was obtained commercially from Crystal Technology in Mountain View, California.

The actual dimensions were $1.9 \times 0.57 \times 0.72$ cm. Crystallographic alignment was accomplished using the X-ray back reflection Laue technique. A typical alignment shot taken normal to the $\langle 100 \rangle$ face is shown in Fig. 4. The sample was wire sawed out of a larger boule and then ground and polished. After final polishing of the end optical faces, the sample was viewed using monochromatic (6328Å) light, as shown in Fig. 5. When monochromatic polarized light was propagated to excite both optical modes, and then examined at the output with a crossed polarizer, an interference pattern (see Fig. 6) resulted which indicated that the sample was slightly wedged. By simultaneously reflecting a laser beam off the front and back surfaces, the wedge angle was found to be approximately 0.3 degrees. This agrees well with the number that is derived by measuring the distance between the fringes, and substituting into the following relations. The phase difference, Γ , between the ordinary and extraordinary mode is given by:

$$\Gamma = \frac{2\pi \ell}{\lambda} (n_e(\text{eff}) - n_o) \quad (108)$$

where λ = optical wavelength, $n_e(\text{eff})$ and n_o are the refractive indices, and ℓ = the interaction length. The phase difference between adjacent fringes is given by:



SC81-13290

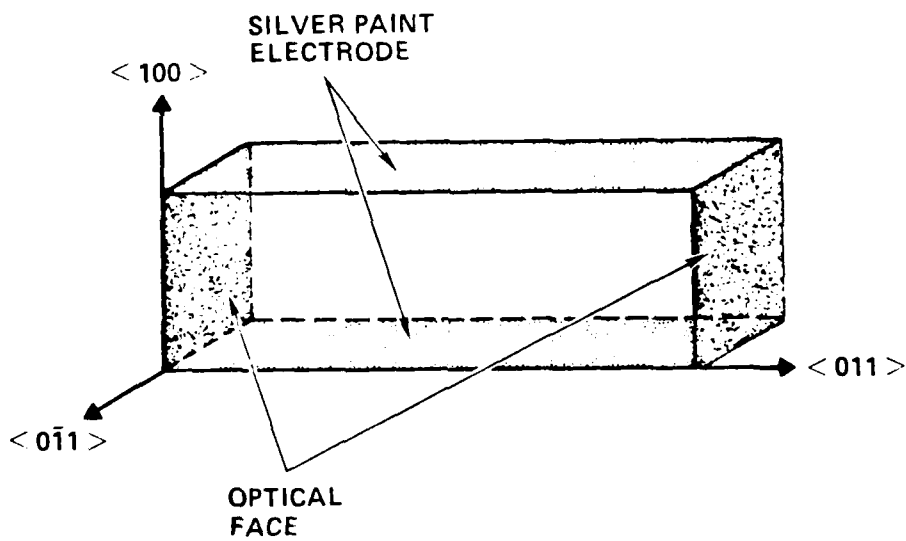


Fig. 3 TeO₂ electro-optic sample configuration.



SC81-14094

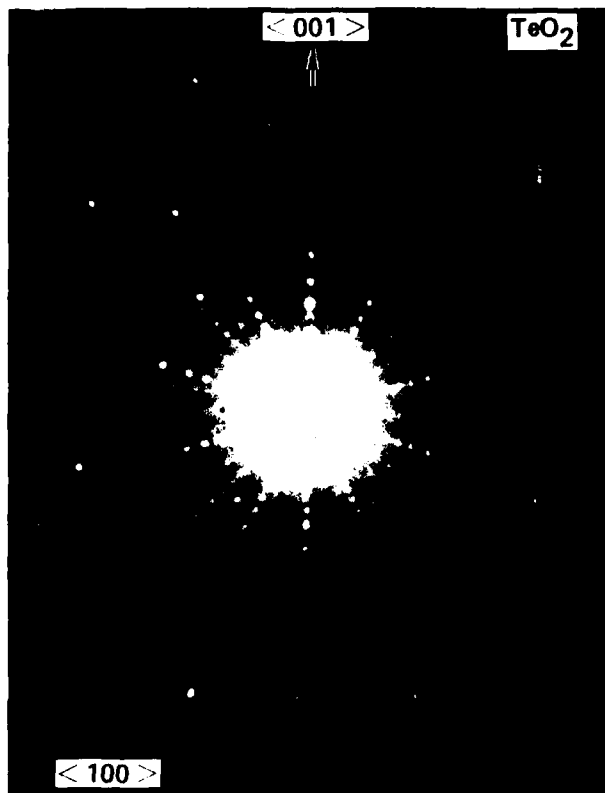


Fig. 4 Laue X-ray photograph of $\langle 100 \rangle$ surface in TeO_2 .



SC5266.1FR

SC81-13291

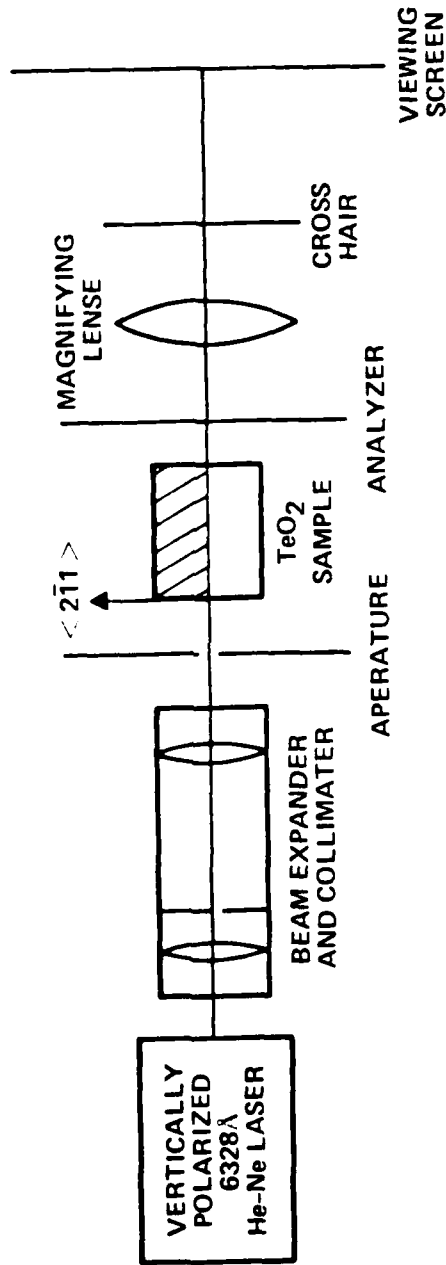


Fig. 5 Optical set-up for electro-optic measurement in TeO_2 .



SC81-13292



Fig. 6 Interference fringe patterns from electro-optic measurement in TeO_2 .



$$\Delta\Gamma = \frac{2\pi}{\lambda} (n_e(\text{eff}) - n_o) (\ell_1 - \ell_2) \quad (109)$$

where ℓ_1 and ℓ_2 are the respective interaction lengths for the two fringes. The absolute phase difference, between adjacent light (or dark) fringes a distance d_0 apart, is π . Further, one can relate the distance between fringes, d_0 , to the wedge angle, α , by:

$$d_0 \approx \frac{\lambda}{2\alpha(n_e(\text{eff}) - n_o)} \quad (110)$$

using the small angle approximation. If the optical path length changes, the fringe pattern will move up or down depending on the sign of the effect. Of course, this change in optical path length may result from either of two different effects: 1) a change in the physical length of the crystal due to mechanical strains induced by the inverse piezoelectric effect and 2) a change in the (extraordinary) index of refraction. We shall show below that the first effect is negligible in TeO_2 . Therefore, assuming that the fringes move only as a result of a change in the index, the distance the fringe pattern moves, d_1 , is given by:

$$d_1 \approx \frac{\lambda}{\alpha} \frac{(n_e'(\text{eff}) - n_e(\text{eff}))}{(n_e(\text{eff}) - n_o)} \quad (111)$$

in the limit of small α . Here $n_e'(\text{eff}) = n_e(\text{eff}) + \Delta n_e(\text{eff})$ with $\Delta n_e(\text{eff}) = -2n_e^3(\text{eff}) r_{41}^T E_x$ where we have assumed that the index has been modified by a dc electric field, E_x . Taking the ratio of d_1/d_0 and solving for r_{41} , we obtain:



$$r_{41}^T = \lambda(d_1/d_0)/(2E_x n_e^3(\text{eff})) \quad (112)$$

All that is required then is to measure the fractional shift in the fringe pattern for a given applied electric field. In order to quantitatively determine this ratio, the sample was placed in the optical setup shown in Fig. 5.

Photographs of the fringe patterns and the fiducial crosshairs for various applied fields are shown in Figs. 6a - 6c. The applied voltages were -4.9, 0 and + 4.9 kV. The result was $d_1/d_0 \approx 1/2$ for 9.8 kV. This corresponds to an index change of $\Delta n_e(\text{eff}) = 8.3 \times 10^{-6}$ and an electro-optic coefficient of $|r_{41}| = 0.76 \times 10^{-12}$ m/V. The sign of this electro-optic coefficient was obtained by correlating the direction of the fringe shift, the wedge angle and the sign of the applied voltage. The result is that $r_{41} = -0.76 \times 10^{-12}$ m/V. The closely spaced fringes in the lower right corners of Figs. 6a - 6c are probably due to a slight rounding of the presumed flat optical face near the edge of the sample.

An estimate of the physical distortion to the sample due to the strain resulting from the inverse piezoelectric effect, is given by the following:

$$e_i = \sum_j d_{ji} E_j \quad (113)$$

where e_i is the strain, d_{ji} is the piezoelectric coefficient and E_j is the applied electric field. The only non-zero piezoelectric coefficient³⁰ for the point group 422 is d_{14} . The measured value²⁷ for TeO_2 is $d_{14} = 8.13 \times 10^{-12}$ C/N. The change in wedge angle resulting from the piezoelectric strain induced by an electric field of 9.8 kV is 0.009° or 0.3% and will, therefore, be neglected.



SC5266.1FR

The strain induced by the inverse piezoelectric effect does, however, affect the index via the strain-optic effect giving rise to a change in impermeability given by:³¹

$$\Delta B_i = \sum_j P_{ij} e_j = \sum_{j,k} P_{ij} d_{kj} E_k \quad (114)$$

where P_{ij} is the relevant component of the photoelastic tensor for TeO_2 . Indeed we may define a secondary electro-optic coefficient by:

$$r_{ik}^{(2)} = \sum_j P_{ij} d_{kj} \quad (115)$$

Since in our experiment $E_k = E_1$ and $d_{kj} = d_{14}$, P_{44} is the only non-zero component which contributes to the secondary E-0 effect. This component has been measured³² and has the value $P_{44} = -0.17$. The secondary E-0 coefficient therefore has the value:

$$r_{41}^{(2)} = P_{44} d_{14} = -1.38 \times 10^{-12} \text{ m/V} \quad (116)$$

Using the applied dc voltage of 9.8 kV, we deduce a change in effective index of

$$\Delta n_e(\text{eff}) = +1.50 \times 10^{-5} \quad (117)$$

If we now subtract this result from the number which was experimentally derived (at constant stress), we obtain



SC5266.1FR

$$\begin{aligned} (\Delta n_e(\text{eff}))_{\text{exp}} - (\Delta n_e(\text{eff}))_{\text{SE-0}} &= 8.3 \times 10^{-6} - 1.5 \times 10^{-5} \\ &= -0.67 \times 10^{-5} \end{aligned} \quad (118)$$

This in turn yields a value for the primary E-0 coefficient at constant strain of:

$$r_{14}^S = +0.62 \times 10^{-12} \text{ m/V} \quad (119)$$

where the superscript S indicates constant strain ("clamped"). This value can be compared with other nonlinear optical measurements in TeO_2 ; for example,

$$|d_{14}^{\text{SHG}}| = 1.45 \times 10^{-9} \text{ esu} = \epsilon_0 \times 0.61 \times 10^{-12} \text{ m/V} \quad (120)$$

derived from second harmonic generation measurements.^{14,15,28,29} (Note that the d_{14} here is distinct from the piezoelectric coefficient referred to above.)

These comparisons should not be made directly between r_{41}^S and d_{14}^{SHG} . Instead they should be made between the electro-optic susceptibility:

$$\chi_{41}^{\text{eo}} = - \frac{n_0^2 n_e^2 r_{41}^S}{4\pi} = -1.5 \times 10^{-12} \text{ m/V} \quad (121)$$

and the second harmonic generation susceptibility d_{14}^{SHG} .



2.2.2 Tl₃AsSe₃

Thallium arsenic selenide or TAS is a ternary semiconductor which crystallizes with the trigonal point group symmetry 3m. This implies that TAS is optically uniaxial and should have 4 non-zero electro-optic components:⁷ r_{13} , r_{22} , r_{33} , and r_{51} . This compound has been the subject of extensive investigation for its optic,³² acousto-optic,³³⁻³⁵ and non-linear³⁶ (second harmonic generation) properties. It is transparent from the near (0.9 μm) to mid (14 μm) IR. By using some of the formalism associated with the dielectric impermeability tensor derived above (Section 2.2.1), we now examine the electro-optic effect in TAS.

As a preliminary example, let us consider the case of an x-y-z rectangular prism cut so that the long dimension is along x. The dc electric field is applied normal to the long direction and along y. The third direction or z, is parallel to the optic axis. Light is then propagated along x and polarized along y (ordinary) or along z (extraordinary). The dielectric impermeability tensor is then:

$$B = \begin{pmatrix} \frac{1}{n_o^2} & 0 & 0 \\ 0 & \frac{1}{n_o^2} + r_{22}E_y & r_{51}E_y \\ 0 & r_{51}E_y & \frac{1}{n_e^2} \end{pmatrix} \quad (122)$$

The off-diagonal components, $r_{51}E_y$, produce a small rotation of the indicatrix about the x axis by an amount:

$$\tan 2\theta = \frac{2r_{51}E_y}{\frac{1}{n_o^2} - \frac{1}{n_e^2} + r_{22}E_y} \quad (123)$$



SC5266.1FR

An upper estimate of this rotation (assuming $r_{22} = 100 \times 10^{-12}$ m/V) for voltages of 5KV is $\theta < 1^\circ$, and, therefore, this effect will be ignored. Light polarized along y (ordinary) has the effective index:

$$n = n_o - \frac{n_o^3 r_{22} E_y}{22} \quad , \quad (124)$$

while the other polarization (along z or extraordinary) remains

$$n = n_e \quad . \quad (125)$$

Therefore, it is only the ordinary component which is affected by the dc field. If we then arrange to have the incident light linearly polarized 45° between y and z, or along $\langle 011 \rangle$, both modes will be excited. Due to the difference in propagation velocities, the two modes will emerge out of phase with one another by an amount, Γ , given by:

$$\Gamma = \frac{2\pi\ell}{\lambda} (\Delta n) \quad (126)$$

where as before ℓ is the interaction length, λ is the wavelength and Δn is the birefringence ($n_e - n_o$). The polarization state at the exit face will be in general elliptical, with circular and linear polarizations as specific cases (for 90° and 0° or 180° phase differences, respectively). As we have shown, if an electric field is applied along y, then the birefringence, and hence, Γ , changes by:



SC5266.1FR

$$\Delta\Gamma = \frac{-2\pi\ell}{\lambda} \frac{n_0^3 E_y r_{22}}{2} \quad (127)$$

The total phase retardation is then

$$\Gamma_0 + \Delta\Gamma = \frac{2\pi\ell}{\lambda} ((\Delta n) - n_0^3 E_y r_{22}) \quad (128)$$

To experimentally observe this effect, we set up the sample and optics as shown in Fig. 7. The laser used was a He-Ne 3.39 μm laser. The compensator was adjusted to give linearly polarized light with no field applied. The polarizer was then "crossed" so that essentially no light was observed at the detector. As the electric field was increased, a series of oscillations in the signal from the detector was observed as the state of the light exiting the crystal changed ellipticity. The voltage required to change the signal by one oscillation (or the phase by π) is called the half-wave voltage V_π and is given by:

$$\Delta\Gamma = \frac{-2\pi\ell}{\lambda} \frac{n_0^3 E_y r_{22}}{2} \quad (129)$$

$$\pi = \frac{-2\pi\ell}{\lambda} \frac{n_0^3 V_\pi r_{22}}{2y} \quad (130)$$

where y is the distance between the electrodes. Letting y and ℓ be of unit dimension:

$$V_\pi = \frac{\lambda}{n_0^3 r_{22}} \quad (131)$$



SC81-14092

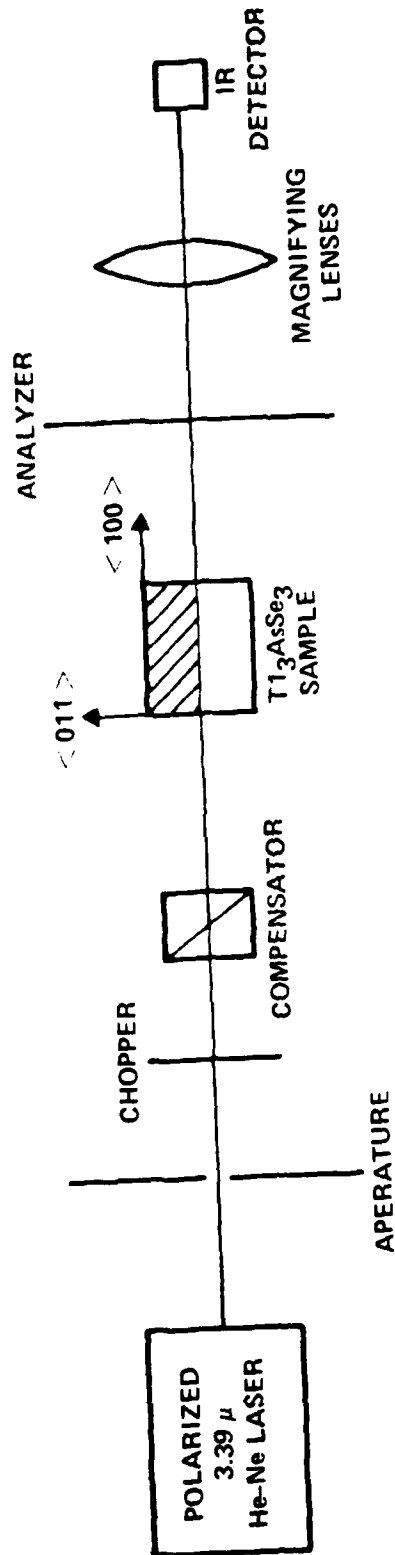


Fig. 7 Optical set-up for electro-optic measurement in Tl₃AsSe₃.



The sample used in this preliminary experiment was fashioned from an in-house grown^{36,37} boule of Tl_3AsSe_3 . The sample was first wire sawed from the boule and then mechanically ground and polished (on the optical faces) to finished dimensions of $0.36 \times 0.32 \times 1.27$ cm for y , z and x , respectively. Silver paint was used for electrodes. The sample resistance with no applied field was greater than 20 Mohm which meant the resistivity was more than 2×10^7 ohm-cm. This is consistent with the room temperature, and an approximately 1 eV band-gap.³⁶ Figure 8 shows the data for this preliminary experiment.

Using the voltage between peaks of 2.2 kV and the sample dimensions of 1.27 cm for z and 0.36 cm for y and the room temperature index at $3.39 \mu m$ of 3.37, we find $r_{22}^T \cong 11 \times 10^{-12}$ m/V, and the half wave voltage $V_{\pi} \cong 8$ kV. This result includes the piezoelectric-induced effects.

Our next experiment, to be carried out under the follow-on to this contract, will be to place the electric field along z , with the same sample geometry as before. The dielectric impermeability tensor then becomes

$$B = \begin{pmatrix} \frac{1}{n_o^2} + r_{13}E_3 & 0 & 0 \\ 0 & \frac{1}{n_o^2} + r_{13}E_3 & 0 \\ 0 & 0 & \frac{1}{n_e^2} + r_{33}E_3 \end{pmatrix} \quad (132)$$

With light propagating along x and polarized along y , (the ordinary mode), the index becomes:

$$n_o' = n_o - \frac{n_o^3 r_{13} E_3}{2} \quad (133)$$

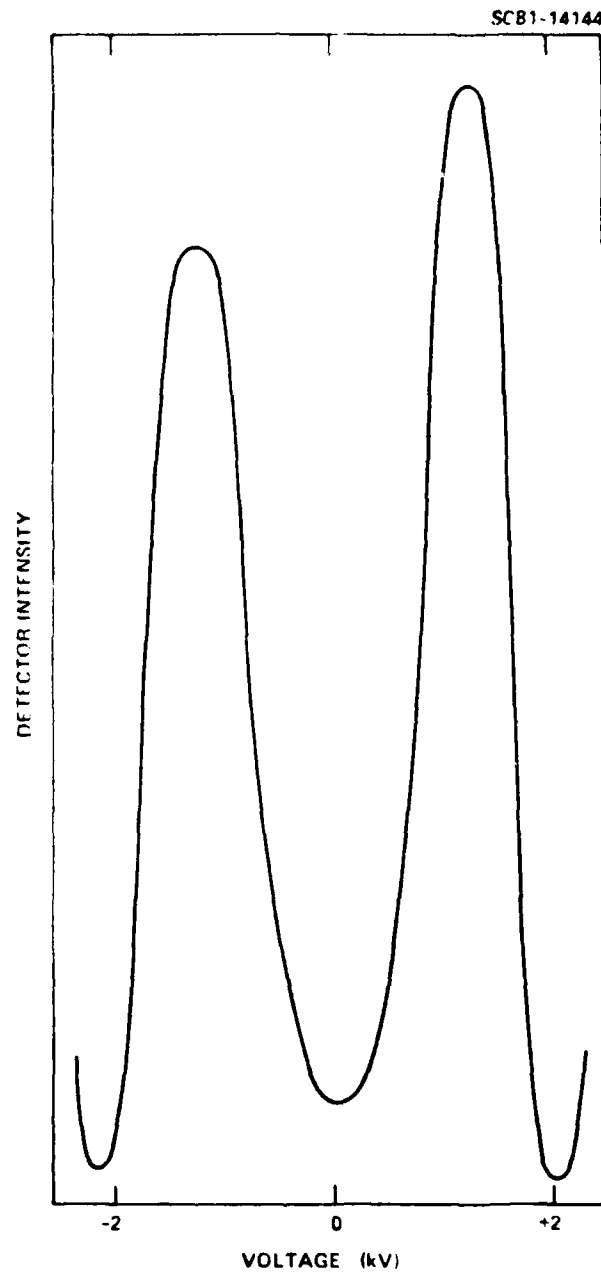


Fig. 8 Plot of detector intensity vs applied voltage from electro-optic measurement in Tl_3AsSe_3 .



SC5266.1FR

The orthogonal polarization along z (the extraordinary mode) has the following index:

$$n_e' = n_e - \frac{n_e^3 r_{33} E_3}{2} \quad (134)$$

It is common practice to define the effective birefringence in terms of a combined electro-optic coefficient r_c :

$$\begin{aligned} \Delta n' &= (n_e - n_o) - \frac{E_3}{2} (n_e^3 r_{33} - n_o^3 r_{13}) \\ &= (n_e - n_o) - \frac{E_3 r_c n_e^3}{2} \end{aligned} \quad (135)$$

with

$$r_c = \frac{1}{2} \left(r_{33} - \frac{n_o^3 r_{13}}{n_e^3} \right) \quad (136)$$

The field dependent phase retardation is then

$$\begin{aligned} \Delta \Gamma &= \frac{2\pi}{\lambda} \times \frac{1}{2} (n_e^3 r_{33} - n_o^3 r_{13}) E_3 \\ &= \frac{2\pi}{\lambda} \times r_c E_3 n_e^3 \end{aligned} \quad (137)$$

The half-wave voltage V_π in this case is:

$$2\pi = \frac{2\pi}{\lambda} \times r_c V_\pi n_e^3 / y \quad (138)$$



SC5266.1FR

$$V_{\pi} = \frac{\lambda}{n_e^3 r_c} \quad (139)$$

for unit sample dimensions.

It will, therefore, be possible to measure r_c using the same experimental arrangement as before, by merely removing the silver paint electrodes from the y-faces and placing them on the z-faces.

The coefficient r_{13} can be independently obtained by a longitudinal measurement on a z-cut plate. The index change seen by light propagating along the z direction polarized in the x-y plane (pure ordinary) is simply:

$$n' = n_0 - \frac{n_0^3}{2} r_{13} E_3 \quad (140)$$

which can be measured in a Fabry-Perot configuration. Then by knowing r_{13} and r_c , we can calculate r_{33} . The coefficient r_{51} can be measured as a rotation of the indicatrix using a longitudinal geometry with propagation along the y axis.

Finally, in order to obtain the "clamped" electro-optic coefficients, r_{ij}^S , it will be necessary to experimentally determine the piezoelectric coefficients and photoelastic constants of Tl_3AsSe_3 .



SC5266.1FR

3.0 SUMMARY AND RECOMMENDATIONS

In summary, this program has advanced well, with significant progress being made on both the theoretical and experimental portions of this program. The groundwork has been established for the theoretical approach to the electro-optic effect in solids. The underlying philosophy to our method is to use a generalized "chemical bond" approach to the first- and second-order electric susceptibility. This methodology utilizes nearest-neighbor interactions, and parametrizes the relevant matrix elements in terms of universal atomic parameters. Calculations, therefore, only require a knowledge of elemental composition and the atomic bond configurations. This approach lends itself to predictive comparisons of electro-optic response not only within a given crystal structure (making elemental substitutions) but between different structures as well.

Details of the methodology associated with the Bond Orbital Model have been given along with applications to the specific cases of the chalcopyrite and zincblende crystal structures. Initially, however, the Bond Orbital Model was only applicable to calculations of the response of the electronic system to probing fields of frequencies above the Restrahl frequency and below the first inter-band or interatomic transition. Therefore, the next level of sophistication introduced into the problem was an attempt to include the lattice dynamics.

The approach here (still being developed) was formulated in terms of the microscopic spring constants. Knowing these spring constants, one could, in principle, calculate the relative displacement and resulting lattice distortion



SC5266.1FR

of a crystal in the presence of a dc electric field. Then, by knowing the new equilibrium ionic positions, one can recalculate the susceptibility and hence the electro-optic effect. The process is evolving along lines oriented towards obtaining these microscopic spring constants from macroscopic measurable properties of the materials such as elastic constants or lattice mode frequencies. This approach tends to somewhat diminish the overall generality and, therefore, predictive properties of the method in that more measurements are required before the calculations may be undertaken. This, however, should not be taken as an end result, but rather as an intermediate step in an evolving process. At some future date, it is hoped also to be able to generalize the lattice response to structure and elemental composition, thereby recovering the predictive capabilities.

The experimental portion of this program has involved measurements of the electro-optic effect in TeO_2 and Tl_3AsSe_3 . The TeO_2 data is complete and has yielded the value $r_{41}^S = -0.51 \times 10^{-12}$ m/V. Experiments on Tl_3AsSe_3 at $3.39 \mu\text{m}$ have just begun but a preliminary result indicates $|r_{22}^T| \approx 11 \times 10^{-12}$ m/V. Further measurements will be carried out on Tl_3AsSe_3 during the next phase of the program to obtain r_{11} and r_{33} . Additionally, other materials such as SbSI and Barium Titanium Niobate (BTN) will be approached experimentally during the next phase of this program. SbSI has one of the highest reported piezoelectric coupling coefficients of any solid,³⁸ and should have a correspondingly large electro-optic effect. BTN has been shown to have a significant electro-optic effect.³⁹ Structural considerations have shown that it may be possible to substitute lanthanum or potassium on some of the sites in the unit cell.



SC5266.1FR

Our recommendation, therefore, is to proceed with the theoretical work to approach a completely generalized formalism which has predictive capabilities. In addition, the experimental work should proceed to evaluate materials which provide insight and feedback to the theory, as well as provide new high performance materials for further applied device efforts.



4.0 REFERENCES

1. W.A. Harrison, Phys. Rev. B8, 4487 (1973).
2. W.A. Harrison and S. Ciraci, Phys. Rev. B10, 1516 (1974).
3. W.A. Harrison, Electronic Structure and the Properties of Solids, (W.H. Freeman & Co., San Francisco, 1980).
4. M.D. Ewbank, P.R. Newman and W.A. Harrison, NBS SP 574, 217 (1980).
5. D.A. Kleinman, Phys. Rev. 126, 1977 (1962).
6. J.F. Nye, Physical Properties of Crystals, (Univ. Press, Oxford, England, 1976) p. 241.
7. I.P. Kaminow and E.H. Turner, in Handbook of Lasers, ed. by R.J. Pressley (Chemical Rubber Co., Cleveland, 1971) p. 447.
8. D.F. Nelson, J. Opt. Soc. Am. 65, 1144 (1975).
9. J.D. Jackson, Classical Electrodynamics, (John Wiley & Sons, Inc., N.Y., 1967) p. 109.
10. W.A. Harrison, op. cit. 3, p. 120.
11. G.D. Boyd and D.A. Kleinman, J. Appl. Phys. 39, 3597 (1968).
12. P.A. Franken and J.F. Ward, Rev. Mod. Phys. 35, 23 (1963).
13. M. Bass, P.A. Franken and J.F. Ward, Phys. Rev. 138, A534 (1965).
14. S. Singh, W.A. Bonner and L.G. VanUitert, Phys. Lett. 38A, 407 (1972).



SC5266.1FR

15. B.F. Levine, IEEE J. Quan. Elec. QE-9, 946 (1973).
16. M.E. Lines and J.V. Waszczak, J. Appl. Phys. 48, 1395 (1977).
17. M.M. Choy, S. Ciraci and R.L. Boyer, IEEE J. Quan. Elec. QE-11, 40 (1975).
18. W.A. Harrison, Festkorperprobleme XVII, 135 (1977).
19. S. Froyen and W.A. Harrison, Phys. Rev. B20, 2420 (1979).
20. W.A. Harrison, "New Tight-Binding Parameters for Covalent Solids Obtained Using Louie Peripheral States," submitted to Phys. Rev. B, May 1981.
21. W.A. Harrison, op. cit. 3, p. 196, p. 208 and p. 220.
22. J. Leciejewicz, Z. Kristallogr. 116, 345 (1961).
23. D.M. Korn, A.S. Pine, G. Dresselhaus, and T.B. Reed, Phys. Rev. B8, 768 (1973).
24. I.J. Fritz, T.J. Isaacs, M. Gottlieb and B. Morosin, Sol. St. Comm. 27, 535 (1978).
25. N. Uchida and Y. Ohmachi, J. Appl. Phys. 40, 4692 (1969).
26. P.S. Peercy, I.J. Fritz and G.A. Samara, J. Phys. Chem. Sol. 36, 1105 (1975).
27. B.A. Auld, Acoustic Fields and Waves in Solids, Vol. 1, (Wiley & Sons, N.Y., 1973) p. 376.
28. D.S. Chemla and J. Jerphagnon, Appl. Phys. Lett. 20, 222 (1972).



SC5266.1FR

29. L.M. Belyaev, A.V. Gil'varg, L.M. Dorozhkin, V.A. Kizel', V.M. Koval'chuk and S.P. Smirnov, JETP Lett. 17, 142 (1973).
30. J.F. Nye, *op. cit.*, p. 124.
31. *ibid.*, p. 244.
32. M.D. Ewbank, P.R. Newman, N.L. Mota, S.M. Lee, W.L. Wolfe, A.G. DeBell and W.A. Harrison, J. Appl. Phys. 51, 3848 (1980).
33. I.C. Chang, Opt. Eng. 16, 455 (1977).
34. M. Gottlieb and G.W. Roland, Opt. Eng. 19, 901 (1980).
35. M. Koshnevisan, R. Hall, E.A. Sovero, E. Skurnick and W. Davidson, Proc. IEEE Ultrasonics Symp. 1, 470 (1980).
36. J.D. Feichtner and G.W. Roland, Appl. Opt. 11, 993 (1972).
37. H. Kuwamoto, "Seeded Growth of Tl_3AsSe_3 ," to be published.
38. D. Berlincourt, H. Jaffe, W.J. Merz and R. Nitsche, Appl. Phys. Lett. 4, 61 (1964).
39. Y. Itoh and H. Iwasaki, J. Phys. Chem. Solids 34, 1639 (1973).

APPENDIX I

LINEAR ELECTRO-OPTIC EFFECT IN TELLURIUM DIOXIDE*

M.D. Ewbank and P.R. Newman

Rockwell International Science Center
1049 Camino dos Rios
Thousand Oaks, CA 91360

ABSTRACT

The only non-zero dc electro-optic (or Pockel's) coefficient in tellurium dioxide was measured at constant stress. The result was $r_{41}^T = -0.76 \times 10^{-12}$ m/V. The secondary electro-optic effect, due to the converse piezoelectric and photoelastic effects, is approximately twice the observed electro-optic response.

*This work was supported by ONR contract number N00014-80-C-0498.

I. INTRODUCTION

Tellurium dioxide (paratellurite or TeO_2) is a well-known acousto-optic material,^{1,2} utilized in devices such as acousto-optic tunable filters,^{3,4} beam deflectors and modulators. The anomalously slow acoustic shear velocity,¹ in the $\langle 110 \rangle$ direction which can be associated with the onset of a soft lattice mode transition,⁵ leads to a favorable acousto-optic figure-of-merit. The presence of nearby phase transitions in ferroelectric materials which exhibit superior electro-optic behavior⁶ suggests that the electro-optic effect in TeO_2 may also be enhanced by this softening lattice mode. Consequently, the room temperature value of the single non-zero dc electro-optic coefficient (r_{41}^T) for TeO_2 was determined experimentally at a wavelength of 6323 Å.

II. EXPERIMENT

The point group symmetry⁷ of tellurium dioxide is 422, which implies that TeO_2 is optically uniaxial and has only two non-zero electro-optic coefficients ($r_{41} = -r_{52}$).⁸ An optical quality sample of TeO_2 was fabricated, using material obtained commercially from Crystal Technology, Inc., with the orientation for the measurement of r_{41} indicated in Fig. 1. The optical faces, 1.9 cm apart, were perpendicular to the $\langle 011 \rangle$ direction, and the silver-painted electrodes, separated by 0.57 cm, were normal to $\langle 100 \rangle$. A schematic of the optical setup is illustrated in Fig. 2. At a wavelength of

6328 Å, TeO_2 is optically transparent and its refractive indices at room temperature⁹ are $n_o = 2.2585$ and $n_e = 2.4112$.

For light propagating in the $\langle 011 \rangle$ direction and polarized in the $\langle 2\bar{1}1 \rangle$ direction (i.e., at 45 degrees from $\langle 100 \rangle$ and $\langle 0\bar{1}1 \rangle$) both the ordinary and extraordinary modes of propagation are equally excited. When the ordinary and extraordinary beams exit the TeO_2 sample, the relative phase shift, Γ , between ordinary and extraordinary beams, assuming that the dc electric field is zero and that the front and back surfaces are exactly flat and parallel, will be

$$\Gamma = (2\pi \ell / \lambda)(n_e(\text{eff}) - n_o) \quad (1)$$

where ℓ is the sample interaction length, λ is the wavelength, and n_o is the ordinary index. The effective index of the extraordinary wave, $n_e(\text{eff})$, for this propagation direction is given by the relation¹⁰

$$n_e(\text{eff}) = \sqrt{2} n_o n_e / \sqrt{n_o^2 + n_e^2} \quad (2)$$

with n_e being the extraordinary index.

Since the ordinary and extraordinary waves have equal amplitudes, the intensity of the analyzed beam will vary with the orientation of the analyzing polarizer, because the polarization state of the unanalyzed light is either linear, elliptic or circular depending on the relative phase retardation of the two modes. If the front and rear surfaces of the sample are wedged

slightly, an interference fringe pattern will result. The spacing, d_0 , between adjacent fringes which have a relative phase shift of π , can be written:

$$d_0 \cong \frac{\lambda}{2\alpha[n_e(\text{eff}) - n_o]} \quad (3)$$

in the limit that the wedge angle, α , is small.

When an external dc electric field, E_x , is applied in the $\langle 100 \rangle$ direction, the extraordinary wave experiences a change in impermeability of $r_{41}^T E_x$, which corresponds to an effective extraordinary index change, $\Delta n_e(\text{eff})$, given by¹⁰

$$\Delta n_e(\text{eff}) \cong -r_{41}^T E_x n_e^3(\text{eff})/2 \quad (4)$$

in the approximation that this change in index is much less than the index itself. The superscript "T" indicates that the measurement is performed under constant stress ("unclamped")⁶. (This change in effective index is maximized for the $\langle 011 \rangle$ propagation direction only in the limit of the birefringence approaching zero. For the birefringence of TeO_2 at 6328 Å, the maximum occurs when propagating about 3 degrees away from the $\langle 011 \rangle$ direction; but the difference in effective index change for these two propagation directions is less than 0.5% and therefore is negligible.) Since the dc electric field does not affect the ordinary wave, the phase shift between ordinary and extraordinary modes will change with external electric field by an amount that

can be determined by combining Eqs. (1) and (4). More specifically, the fringe pattern will shift by a distance, d_1 , when the dc field is applied:

$$d_1 \cong \frac{\lambda [n'_e(\text{eff}) - n_e(\text{eff})]}{\alpha [n'_e(\text{eff}) - n_o]} \quad (5)$$

where $n'_e(\text{eff})$ is the effective extraordinary index for a non-zero dc field (i.e., $n'_e(\text{eff}) = n_e(\text{eff}) + \Delta n_e(\text{eff})$). The fringe shift with respect to the separation between fringes can then be written as the ratio:

$$(d_1/d_0) \cong 2\lambda \Delta n_e(\text{eff})/\lambda \quad (6)$$

in the approximation that the change in effective extraordinary index is much less than the effective birefringence, $[n_e(\text{eff}) - n_o]$. Finally, the electro-optic coefficient, r_{41}^T , can be expressed as a function of this fractional fringe shift, the external dc electric field, the wavelength, the sample interaction length and the effective extraordinary refractive index in the following form:

$$r_{41}^T \cong \frac{-\lambda (d_1/d_0)}{2E_x n_e^3(\text{eff})} \quad (7)$$

Voltages of -4.9, 0.0 and +4.9 kV were supplied to the electrodes on the x-faces of the TeO_2 sample and produced the interference fringe patterns shown in Fig. 3. The relative motion of the fringes, or fractional fringe

shift, was determined, from photographic measurements referenced to a fixed cross-hair, to be approximately 1/2 fringe ($\pm 20\%$) for an applied voltage change of 9.8 kV. It should be noted that the closely spaced fringes in the lower right corners of Figs. 3a, b, and c are probably due to a slight rounding of the presumed flat optical face near one edge of the sample. Additionally, the fine rectangular fringe pattern is caused by Fresnel diffraction from the sample aperture. The wedge angle was found, by comparing simultaneous reflections from both optical faces, to be approximately 0.3 degrees, which is roughly consistent with the number of major fringes shown in Fig. 3. Since the wedge angle is so small, Eq. (7) has been used to calculate a room temperature value for the magnitude of the electro-optic coefficient of TeO_2 at 6328 Å, which was $|r_{41}^T| = 0.76 \times 10^{-12}$ m/V. Equation (4) indicates that this corresponds to an effective extraordinary index change of $\Delta n_e(\text{eff}) = 8.3 \times 10^{-6}$.

The sign of this electro-optic coefficient was obtained by correlating the direction of fringe shift with respect to the sign of applied voltage and the orientation of the wedge angle with respect to the optic axis. The orientation of the optic axis was determined by noting that, for this direction of propagation, the extraordinary beam experienced a "walk-off", with respect to the ordinary beam, of 3.7 degrees in the direction of the optic axis. Referring to the fringe patterns in Fig. 3, the electrodes lie on the faces perpendicular to the fringes, with the ground electrode being on the upper right face. The wedging, as determined by retroreflection, indicated that the interaction length in the portion of the sample, which corresponds to

the region near the upper left surface of Fig. 3, is longer than the interaction length near the lower right surface. When a positive voltage was applied to the lower left face, the fringes shifted toward the lower right where the interaction length has decreased. In order to maintain a constant phase difference for a given fringe, the optical path length must remain the same. Since the physical path length decreased for a positive voltage, the index apparently increased to yield a constant optical path length. Then, by utilizing Eq. (4), the electro-optic coefficient, r_{41}^T , must be negative.

Finally, the results of this electro-optic measurement on TeO_2 at 6328 Å can be summarized as

$$r_{41}^T = -0.76 \times 10^{-12} \text{ m/V} \quad (8)$$

for the room temperature value.

III. DISCUSSION

The above experiment with TeO_2 measures relative changes in optical path lengths between ordinary and extraordinary waves, caused by the application of an external dc electric field. However, three physical phenomena can result in a change in the optical path length: (1) the electro-optic effect which directly changes the refractive index, (2) the converse piezoelectric effect which changes the physical dimensions of the crystal (in particular, the angle), and (3) the secondary electro-optic effect (the photoelastic

or strain-optic effect due to the converse piezoelectric, induced strain) which also modifies the refractive index.

The strain, e_i , which results from the converse piezoelectric effect, can be calculated by using the relation:¹¹

$$e_i = \sum_j d_{ji} E_j \quad (9)$$

where d_{ji} is the piezoelectric coefficient and E_j is the electric field. The physical deformation can then be estimated from the measured value of the only non-zero piezoelectric coefficient¹² ($d_{14} = 8.13 \times 10^{-12}$ C/N) and the external dc electric field. This shear strain corresponds to a change in wedge angle of approximately 0.3% for an applied voltage change of 9.8 kV and a negligible fringe shift.

The secondary electro-optic effect gives rise to a change in impermeability, ΔB_i , given by¹³

$$\Delta B_i = \sum_j p_{ij} e_j = \sum_{j,k} p_{ij} d_{kj} E_k \quad (10)$$

where p_{ij} is the photoelastic constant, e_j is the piezoelectric strain, d_{kj} is the piezoelectric coefficient and E_k is the electric field. Then, the secondary electro-optic coefficient, $r_{ik}^{(2)}$, can be defined by the equation

$$r_{ik}^{(2)} = \sum_j p_{ij} d_{kj} \quad (11)$$

Since d_{14} is the only non-zero piezoelectric coefficient, only p_{44} contributes to $r_{ik}^{(2)}$ in Eq. (11), and this photoelastic constant has been found experimentally¹ ($p_{44} = -0.17$). The secondary electro-optic coefficient is -1.38×10^{-12} m/V, which corresponds to a change in effective extraordinary index of $\Delta n_e(\text{eff}) = +1.50 \times 10^{-5}$ using an equivalent form to Eq. (4) with a 1.7×10^6 V/m electric field. Subtracting this secondary electro-optic coefficient from the measured value at constant stress (see Eq. (8)), one obtains the primary¹³ electro-optic coefficient for TeO_2 :

$$r_{41}^S = +0.62 \times 10^{-12} \text{ m/V} \quad (12)$$

where the superscript "S" indicates constant strain ("clamped").⁶

There have been numerous measurements of the second harmonic generation (SHG) coefficient in TeO_2 ^{9,14-16} which have shown a violation of Kleinman's symmetry relation.¹⁷ The results of these measurements yield a reasonably consistent value of approximately

$$|d_{14}| = 1.45 \times 10^{-9} \text{ esu} = \epsilon_0 \times 0.61 \times 10^{-12} \text{ m/V} \quad (13)$$

for a fundamental wavelength of $1.064 \mu\text{m}$, and where ϵ_0 is the permittivity of free space. Note that this d_{14} is distinct from the piezoelectric coefficient in Eqs. (9)-(11). In addition, both the symmetric and antisymmetric nonlinear optical susceptibilities for sum and difference mixing have

been measured in TeO_2 , and the symmetric coefficient is in good correspondence with the SHG value in Eq. (13).¹⁸

Previous attempts have correlated the second order susceptibilities of optical rectification and the linear electro-optic effect.¹⁹ Also, comparison with SHG have been made,^{21,23} but only when absorption and dispersion are negligible (i.e., the same conditions for Kleinman's symmetry¹⁷). These comparisons should not be made directly between r_{41}^S and d_{14}^{SHG} . Instead, they should be done between the electro-optic susceptibility,¹⁹

$$\chi_{41}^{\text{eo}} = \frac{-n_o^2 n_e^2 r_{41}^S}{4\pi} = -1.5 \times 10^{-12} \text{ m/V} \quad , \quad (14)$$

and the second harmonic susceptibility, d_{14}^{SHG} . Since a non-zero SHG coefficient for TeO_2 violates Kleinman's symmetry, the necessary assumptions about absorption and dispersion must be inappropriate and, hence, the relationship between the electro-optic and SHG coefficients for TeO_2 is not straightforward.

Qualitatively, the SHG coefficient, while being non-zero, is still recognized as being small in magnitude when compared to other materials. As a consequence, the electronic contribution to the electro-optic effect is assumed to be approximately zero. Then, since the measured electro-optic coefficient is also small, the conclusion is that the expected soft-mode enhancement of the ionic contributions to the electro-optic susceptibility does not occur.

IV. ACKNOWLEDGEMENTS

The sample alignment and fabrication by R.L. Hall was greatly appreciated as were the helpful discussions with W.J. Gunning, P.A. Yeh and W.A. Harrison.

V. REFERENCES

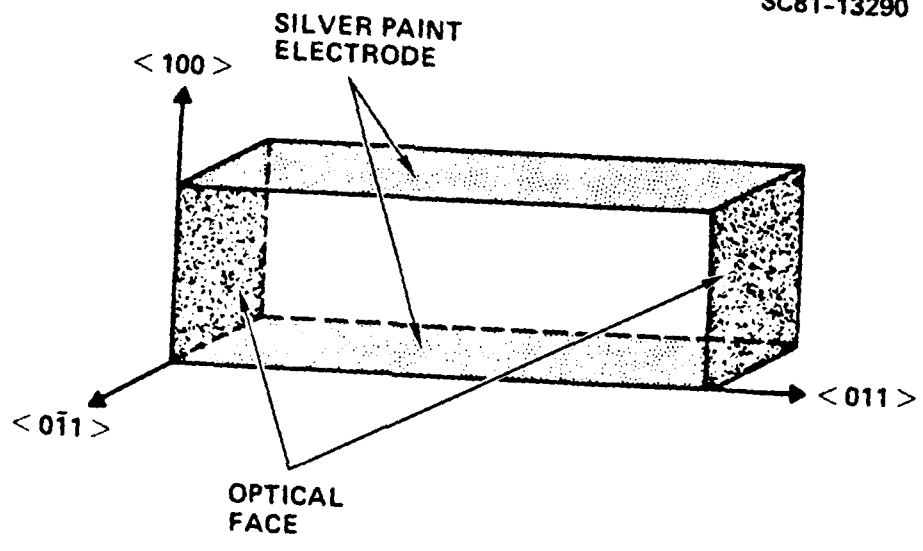
1. N. Uchida and Y. Ohmachi, J. Appl. Phys. 40, 4692 (1969).
2. T. Yano and A. Watanabe, J. Appl. Phys. 45, 1243 (1974).
3. I.C. Chang, IEEE Trans. Sonics Ultrasonics, SU-23, 2 (1976).
4. M. Khoshnevisan, E. Sovero, P.R. Newman and J. Tracy, SPIE, Vol. 245, Cryogenically Cooled Sensor Technology, 63 (1980).
5. P.S. Peercy, I.J. Fritz and G.A. Samara, J. Phys. Chem. Sol. 36, 1105 (1975).
6. I.P. Kaminow and E.H. Turner, in Handbook of Lasers, ed. by R.J. Pressley (Chemical Rubber Co., Cleveland, 1971) p. 447.
7. J. Leciejewicz, Z. Kristallogr., 116, 345 (1961).
8. J.F. Nye, Physical Properties of Crystals, (Univ. Press Oxford, Eng., 1976), p. 124.
9. S. Singh, W.A. Bonner and L.G. Van Uitert, Phys. Lett. 38A, 407 (1972).
10. D.F. Nelson, J. Opt. Soc. Am. 65, 1144 (1975).
11. J.F. Nye, op. cit., p. 115.

12. B.A. Auld, Acoustic Fields and Waves in Solids, Vol. 1, (Wiley & Sons, N.Y., 1973), p. 376.
13. J.F. Nye, op. cit., pp. 244-245.
14. D.S. Chelma and J. Jerphagnon, Appl. Phys. Lett. 20, 222 (1972).
15. L.M. Belyaev, A.V. Gil'varg, L.M. Dorozhkin, V.A. Kizel', V.M. Koval'chuk and S.P. Smirnov, JETP Lett. 17, 142 (1973).
16. B.F. Levine, IEEE J. Quan. Elec. QE-9, 946 (1973).
17. D.A. Kleinman, Phys. Rev. 126, 1977 (1962).
18. M. Okada, K. Takizawa and S. Ieiri, J. Appl. Phys. 48, 4163 (1977).
19. M. Bass, P.A. Franken and J.F. Ward, Phys. Rev. 133, A534 (1965).
20. J.F. Ward, Phys. Rev. 143, 569 (1966).
21. J.F. Ward and P.A. Franken, Phys. Rev. 133, A183 (1964).
22. R.C. Miller, Appl. Phys. Lett. 5, 17 (1964).
23. J.F. Ward and G.H.C. New, Proc. Roc. Soc. A299, 238 (1967).

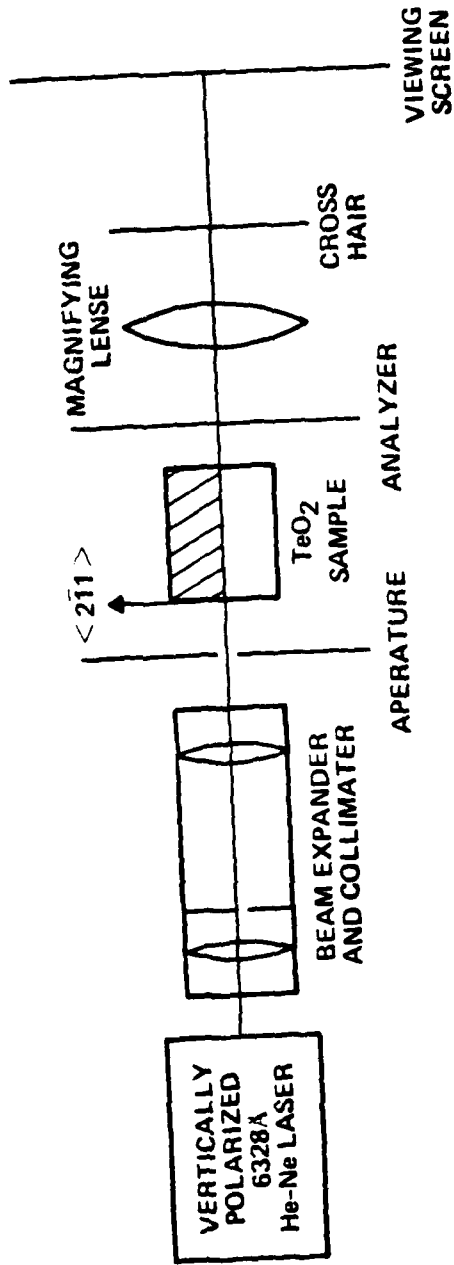
VI. LIST OF FIGURES

1. Crystal orientation for TeO_2 electro-optic sample.
2. Optical configuration of electro-optic measurement.
3. Interference fringe patterns in TeO_2 for (a) -4.9, (b) 0.0 and (c) +4.9 kV.

SC81-13290



SC81-13291



SCB-13292



(a)



(b)



(c)